

Effective Constraints and Physical Coherent States in Quantum Cosmology: A Numerical Comparison

Martin Bojowald* and Artur Tsobanian†

Institute for Gravitation and the Cosmos,
The Pennsylvania State University,
104 Davey Lab, University Park, PA 16802, USA

Abstract

A cosmological model with a cyclic interpretation is introduced, which is subject to quantum back-reaction and yet can be treated rather completely by physical coherent state as well as effective constraint techniques. By this comparison, the role of quantum back-reaction in quantum cosmology is unambiguously demonstrated. Also the complementary nature of strengths and weaknesses of the two procedures is illustrated. Finally, effective constraint techniques are applied to a more realistic model filled with radiation, where physical coherent states are not available.

1 Introduction

To understand the generic behavior of a quantum system, effective equations¹ are useful. In contrast to individual wave functions, or even just stationary states, they directly provide (approximate) equations for time-dependent expectation values. Since the dynamics of expectation values depends on the whole motion of a state — by quantum back-reaction, all moments of a state couple to the expectation values — these equations in general differ from the classical ones by quantum corrections. If quantum corrections, for instance an effective potential, can be found explicitly, an interpretation of quantum dynamics in generic terms becomes much easier. Such results are more general compared to conclusions based on individual states.

Especially in quantum cosmology, the ability to draw generic conclusions is important. Not much is known about the state of the universe except, perhaps, that it currently can well be considered semiclassical. But semiclassicality is not a sharp notion, and so wide classes of states, differing for instance by the sizes of their quantum fluctuations

*e-mail address: bojowald@gravity.psu.edu

†e-mail address: axt236@psu.edu

¹We use the term “effective equations” in a general sense to encompass equations that might follow from an effective action, or be derived in a canonical way. Systematic procedures exist for both ways, and the results agree in cases where they have been explicitly applied [1, 2].

or correlations, are still allowed. In any such situation, a generic analysis is called for, most crucially when long-term evolution is involved, or when one evolves toward strong-curvature regimes such as the big bang singularity where quantum effects of all kinds are expected to be important.

It is sometimes suggested, at least implicitly (and especially in the context of loop quantization), that quantum cosmology might somehow be different from other quantum systems, and that quantum back-reaction could be ignored in its effective equations. Quantum back-reaction might be weak for certain states or in certain regimes, especially for models close to solvable ones, but this observation cannot be generalized. Like the harmonic oscillator in quantum mechanics, there are harmonic cosmologies [3, 4] where expectation values of states follow exactly the trajectories of a corresponding classical system. Such systems are entirely free of quantum back-reaction. For “small anharmonicity”, quantum back-reaction might still be weak, as it is realized in quantum cosmology for matter dominated by its kinetic energy density [5]. But the tough reality of stronger deviations from the solvable ideal of harmonic systems can introduce severe quantum back-reaction, which must be studied in an unbiased and systematic way.

Here, we introduce a model of quantum cosmology which is not solvable but still treatable by two rather different methods: effective constraints and physical states. The model is an anisotropic cosmology of locally rotationally symmetric (LRS) Bianchi I symmetry type, filled with an isotropic, slightly sub-stiff fluid of negative energy density $\rho(a) \propto -\log(a)^2/a^6$ where a is the average scale factor of the anisotropic geometry. With this specific density, the model becomes treatable by physical coherent states, which justifies its contrived and exotic form. Effective constraint techniques [6, 7], applicable much more widely, do not require such a tailored matter source; they are considerably more powerful. As we will see by the explicit comparison of this paper, they capture the information in semiclassical physical states to an excellent degree. Moreover, effective techniques self-consistently determine their ranges of validity. The general applicability of effective constraints will be demonstrated by our final analysis of a model whose matter content, more realistically, is pure radiation.

2 The model

An anisotropic Bianchi I model has a line element

$$ds^2 = -dt^2 + \sum_{I=1}^3 a_I(t)^2 (dx^I)^2$$

with three independent scale factors $a_I(t)$ as functions of proper time t . For a canonical formulation, we denote the momenta of $h_I := a_I^2$ by π^I . It is convenient to introduce Misner variables $(\alpha, \beta_+, \beta_-)$ and their momenta (p_α, p_+, p_-) by the canonical transformation [8]

$$\frac{1}{2} \log(h_1/a_0^2) =: \alpha + \beta_+ + \sqrt{3}\beta_- \quad , \quad 2h_1\pi^1 =: \frac{1}{3}p_\alpha + \frac{1}{6}p_+ + \frac{1}{2\sqrt{3}}p_- \quad (1)$$

$$\frac{1}{2} \log(h_2/a_0^2) =: \alpha + \beta_+ - \sqrt{3}\beta_- \quad , \quad 2h_2\pi^2 =: \frac{1}{3}p_\alpha + \frac{1}{6}p_+ - \frac{1}{2\sqrt{3}}p_- \quad (2)$$

$$\frac{1}{2} \log(h_3/a_0^2) =: \alpha - 2\beta_+ \quad , \quad 2h_3\pi^3 =: \frac{1}{3}p_\alpha - \frac{1}{3}p_+ . \quad (3)$$

In these definitions, a_0 is a reference scale factor (e.g. $a_0 = \sqrt{h_1 h_2 h_3}$ at one moment of time) introduced to be insensitive to coordinate rescalings.

Canonical dynamics in general relativity is determined by the Hamiltonian constraint

$$C_{\text{grav}} = \frac{\pi_{ab}\pi^{ab} - \frac{1}{2}(\pi^a_a)^2}{\sqrt{\det h}} - \frac{\sqrt{\det h}}{(16\pi G)^2} {}^{(3)}R = 0 \quad (4)$$

with the spatial metric h_{ab} , its Ricci scalar ${}^{(3)}R$ and its momenta π^{ab} . Reduced to Bianchi I metrics in Misner variables, specified to a lapse function $N = \sqrt{\det h} = a_1 a_2 a_3$, it simplifies considerably to the form

$$C_{\text{Bianchi I}} = \frac{1}{24}(-p_\alpha^2 + p_+^2 + p_-^2) . \quad (5)$$

As one can check directly, the constraint generates the correct Hamiltonian equations of motion in coordinate time, from which the Kasner solutions follow.

We now restrict the model further by requiring the anisotropy parameter β_- and its momentum p_- to vanish: $\beta_- = 0 = p_-$. In this way, which can easily be confirmed to be consistent with the equations of motion, we enhance the symmetry and leave two independent gravitational variables: the logarithm of the average scale factor, α , and one anisotropy parameter β_+ . The resulting Hamiltonian constraint is equivalent to that of a free, massless relativistic particle.

To introduce a ‘‘potential’’, we will work with a matter source whose energy density is

$$\rho = -\rho_0 \frac{\log(a/a_0)^2}{(a/a_0)^6} = -\rho_0 a_0^6 e^{-6\alpha} \alpha^2 \quad (6)$$

where, in addition to a_0 already introduced, ρ_0 is the matter energy density at some ‘‘initial’’ time. In the presence of matter, its density multiplied with a^6 is to be added to the constraint (5). It becomes²

$$C_{\text{LRS}} = -p_\alpha^2 + p_+^2 - \alpha^2 \nu \quad (7)$$

if we make convenient (and irrelevant) choices for the prefactors and define $\nu = \rho_0 a_0^6$. Our constraint then becomes that of a ‘‘relativistic harmonic oscillator’’ as studied in [7]:

$$p_+^2 = p_\alpha^2 + \nu \alpha^2 . \quad (8)$$

²If we introduce a finite region of coordinate size V_0 to integrate out homogeneous quantities such as the symplectic form $\int d^3x \delta h_{ab} \wedge \delta \pi^{ab} = V_0 \delta h_I \wedge \delta \tilde{\pi}^I = \delta h_I \wedge \delta \pi^I$, the momenta $\pi^I = V_0 \tilde{\pi}^I$ depend on the rather arbitrary V_0 . The lapse function as chosen here would then be homogeneous in V_0 , too, such that $V_0^2 a^6 \rho$ is the matter contribution to the constraint. With this, all its terms scale in the same way if V_0 is changed. Solving the constrained system, we obtain the same reduced phase space for all choices of V_0 .

In this analogy, we consider β_+ as our time variable, and p_+ as the corresponding “energy.” Evolution of α and p_α with respect to β_+ is then generated by the Hamiltonian $p_+ = \pm\sqrt{p_\alpha^2 + \nu\alpha^2}$.

A more realistic matter content could be chosen as radiation, with an energy density $\rho \propto a^{-4} = e^{-4\alpha}$. Here, the Hamiltonian is $p_+ = \pm\sqrt{p_\alpha^2 - \nu e^{2\alpha}}$.

2.1 Classical behavior

We define $H = \sqrt{p_\alpha^2 + \nu\alpha^2}$, such that our constraint solved for p_+ takes the deparameterized form

$$C_{\text{deparameterized}} = p_+ \pm H(\alpha, p_\alpha) = 0.$$

(From now on we choose p_+ positive, to be specific.) This constraint generates Hamiltonian equations of motion for the anisotropies $\dot{p}_+ = 0$ and $\dot{\beta}_+ = 1$, allowing us to identify the time parameter along its flow with β_+ as an internal time. All derivatives in Hamiltonian equations of motion are then with respect to β_+ , specifically

$$\frac{d\alpha}{d\beta_+} = \{\alpha, H\} = \frac{p_\alpha}{H} \quad , \quad \frac{dp_\alpha}{d\beta_+} = \{p_\alpha, H\} = -\frac{\nu\alpha}{H}.$$

Since $H = \mp p_+$ is constant in β_+ , we can combine these equations to a second order one for $\alpha(\beta_+)$, $d^2\alpha/d\beta_+^2 = -\nu\alpha/H^2$ solved by

$$\alpha(\beta_+) = A \sin(\beta_+ \sqrt{\nu}/H) + B \cos(\beta_+ \sqrt{\nu}/H) \quad (9)$$

with integration constants A and B . The equation of motion for α_+ tells us that

$$p_\alpha(\beta_+) = \sqrt{\nu} (A \cos(\beta_+ \sqrt{\nu}/H) - B \sin(\beta_+ \sqrt{\nu}/H)) . \quad (10)$$

With this, the integration constants can be related to H by $H^2 = \nu(A^2 + B^2)$. Solutions in phase space are ellipses of axis lengths $H = |p_+|$ and $\sqrt{\nu}H$, traversed in time β_+ with frequency $(2\pi H/\sqrt{\nu})^{-1}$.

To derive the behavior with respect to proper time, we use the original constraint C_{LRS} not yet deparameterized, and remember that we chose a lapse function $N = a_1 a_2 a_3 = a_0^3 e^{3\alpha}$. Thus, the equation of motion for β_+ with respect to proper time τ is

$$\frac{d\beta_+}{d\tau} = \{\beta_+, e^{-3\alpha} C_{\text{LRS}}\} = 2e^{-3\alpha} p_+ a_0^{-3}.$$

From here, we determine proper time as a function of β_+ by integrating

$$\tau = \frac{a_0^3}{2p_+} \int e^{3\alpha(\beta_+)} d\beta_+ \quad (11)$$

with our solution $\alpha(\beta_+)$. Inverting the solution allows us to insert $\beta_+(\tau)$ into $\alpha(\beta_+)$ and $p_\alpha(\beta_+)$, resulting in solutions as functions of proper time.

It is not easy to integrate $\tau(\beta_+)$ explicitly, but it is clear from the integrand that $\tau(\beta_+)$ is a monotonic, one-to-one function which can be inverted globally. Thus, $\alpha(\tau)$ and $p_\alpha(\tau)$ are defined and finite for all values of proper time. There is no singularity in this model. Clearly, the negative amount of matter energy violates energy conditions sufficiently strongly to provide the cyclic bouncing solutions embodied by ellipses in the (α, p_α) -plane.

One can see this directly from the Friedmann-type equation resulting from the Hamiltonian constraint. We have $p_\alpha^2 = p_+^2 - \nu\alpha^2$, where p_+ is constant and p_α can be obtained from the equation $d\alpha/d\tau = \{\alpha, a_0^{-3}e^{-3\alpha}C_{\text{LRS}}\} = -2a_0^{-3}e^{-3\alpha}p_\alpha$, relating it to the derivative of α by proper time τ . Thus, the constraint equation reads

$$\frac{1}{4}a_0^6e^{6\alpha} \left(\left(\frac{d\alpha}{d\tau} \right)^2 - \frac{4}{a_0^6e^{6\alpha}}(p_+^2 - \nu\alpha^2) \right) = 0$$

and for $a = a_0 \exp(\alpha)$ implies

$$\left(\frac{\dot{a}}{a} \right)^2 = \frac{4p_+^2}{a^6} - 4\rho_0 \frac{(\log a/a_0)^2}{(a/a_0)^6}. \quad (12)$$

On the right hand side, we identify $4p_+^2/a^6$ as the anisotropic shear term, and the contribution $-4\rho_0 a_0^6 (\log a/a_0)^2/a^6$ as our exotic energy density.

The Friedmann equation shows when \dot{a} can vanish, which is realized for $\log a/a_0 = \pm p_+/\sqrt{\nu}$, two solutions which correspond to the maximal and minimal α along our circles. The extrema indeed give us a maximum for $\log a/a_0 = p_+/\sqrt{\nu}$ and a minimum for $\log a/a_0 = -p_+/\sqrt{\nu}$: The sign of \ddot{a} , by the Raychaudhuri equation, is determined by the sign of $\rho + 3P$ of all the matter sources combined. Here, pressure is obtained from the energy density as the negative derivative of energy by volume, i.e. by

$$P = -\frac{\partial E}{\partial V} = -\frac{d(a^3\rho(a))}{3a^2 da} \quad (13)$$

resulting in $P_{\text{neg}} = \rho_{\text{neg}}(1 - \frac{2}{3}(\log a/a_0)^{-1})$ for the negative energy fluid with $\rho_{\text{neg}} = -4\nu(\log a/a_0)^2/a^6$, and $P_{\text{shear}} = \rho_{\text{shear}}$ for the shear contribution with $\rho_{\text{shear}} = 4p_+^2/a^6$. For $\rho + 3P$, this gives

$$\rho + 3P = \rho_{\text{neg}} \left(4 - \frac{2}{\log(a/a_0)} \right) + 4\rho_{\text{shear}}$$

which at the extrema $\log a/a_0 = \pm p_+/\sqrt{\nu}$ evaluates to $\pm 8\sqrt{\nu}p_+/a^6$. The extrema provide a maximum at $\log a/a_0 = p_+/\sqrt{\nu}$ and a minimum at $\log a/a_0 = -p_+/\sqrt{\nu}$, and the evolution is that of a cyclic model with infinitely many bounces and recollapses.

For the model with radiation, we have equations of motion $d\alpha/d\beta_+ = p_\alpha/H$ and $dp_\alpha/d\beta_+ = \nu e^{2\alpha}/H$, with H still constant. The second order equation for $\alpha(\beta_+)$ becomes $d^2\alpha/d\beta_+^2 = \nu e^{2\alpha}/H^2$. For the solution of this model, see Section 4.

2.2 Quantum representation

To represent the model as a quantum system, we start with the obvious kinematical Hilbert space $L^2(\mathbb{R}^2, d\alpha d\beta_+)$ of square integrable wave functions of two variables, β_+ and α . The momentum operators are derivatives times $-i\hbar$, as usual. To arrive at observable information and physical states, we have to implement the constraint operator³

$$\hat{C} = \hat{p}_+^2 - \hat{p}_\alpha^2 - \hat{\alpha}^2 = -\hbar^2 \frac{\partial^2}{\partial^2 \beta_+} + \hbar^2 \frac{\partial^2}{\partial^2 \alpha^2} - \alpha^2, \quad (14)$$

find its kernel and equip it with a physical inner product.

To analyze the quantum constraint, we reformulate it in a first-order way in our time variable β_+ by taking a square root:

$$-\frac{\hbar}{i} \frac{d}{d\beta_+} \Psi(\alpha, \beta_+) = \pm (\hat{p}_\alpha^2 + \hat{\alpha}^2)^{\frac{1}{2}} \Psi(\alpha, \beta_+) =: \pm \hat{H} \Psi(\alpha, \beta_+), \quad (15)$$

introducing the deparametrized Hamiltonian operator $\hat{H} = (\hat{p}_\alpha^2 + \hat{\alpha}^2)^{1/2}$. All solutions of this equation can be expressed as

$$\Psi_\pm(\alpha, \beta_+) = \sum_{n=0}^{\infty} c_n \varphi_n(\alpha) \exp(\mp i \lambda_n \beta_+ / \hbar) \quad (16)$$

where φ_n are the eigenstates of \hat{H} with eigenvalues $\hbar \lambda_n$. Since \hat{H} is the square root of the (positive definite) harmonic oscillator Hamiltonian (with “mass” $m = 1/2$ and “frequency” $\omega = 2$), its eigenstates are of the well-known form, with eigenvalues $\lambda_n = \sqrt{(2n+1)\hbar}$.

In (16), the subscript \pm indicates the sign taken when solving for p_+ by a square root. Solutions naturally split into two classes, positive-frequency solutions Ψ_+ and negative-frequency solutions Ψ_- . The separation into two classes becomes relevant when we introduce the inner product

$$(\Psi, \Phi)_{\text{aux}} := i \int d\alpha \left(\Psi^*(\alpha, \beta_+) \frac{\partial}{\partial \beta_+} \Phi(\alpha, \beta_+) - \Phi(\alpha, \beta_+) \frac{\partial}{\partial \beta_+} \Psi^*(\alpha, \beta_+) \right) \quad (17)$$

of Klein–Gordon form. Although β_+ appears on the right hand side, the inner product evaluated on solutions (16) is time independent. However, $(\cdot, \cdot)_{\text{aux}}$ is not positive definite: it is positive for positive-frequency solutions, but negative for negative-frequency solutions. A positive-frequency solution is automatically orthogonal to a solution with the sign of its frequency flipped. To correct the sign, we define the physical inner product as

$$\langle \Psi, \Phi \rangle := \begin{cases} (\Psi, \Phi)_{\text{aux}} & \text{if } \Psi \text{ and } \Phi \text{ are positive-frequency} \\ -(\Psi, \Phi)_{\text{aux}} & \text{if } \Psi \text{ and } \Phi \text{ are negative-frequency} \\ 0 & \text{otherwise} \end{cases} \quad (18)$$

³Henceforth, for this model, we drop ν for simplicity. It can be absorbed into the variables by first dividing the constraint throughout by $\sqrt{\nu}$, followed by the canonical transformation $\alpha' = \nu^{\frac{1}{4}} \alpha$, $p'_\alpha = \nu^{-\frac{1}{4}} p_\alpha$, $\beta'_+ = \nu^{\frac{1}{4}} \beta_+$, $p'_+ = \nu^{-\frac{1}{4}} p_+$.

and extend it linearly to superpositions of positive and negative frequency solutions. (Alternatively, we may declare positive and negative frequency solutions, respectively, to define two superselection sectors. The procedure here is analogous to [9].) This completes the construction of the physical Hilbert space.

From physical states, β_+ -dependent expectation values (or moments) can be computed, playing the role of evolving observables. As with the non-relativistic harmonic oscillator, this is most easily done using ladder operators: $\hat{\alpha} = \sqrt{\hbar/2} (\hat{a}^\dagger + \hat{a})$, $\hat{p}_\alpha = i\sqrt{\hbar/2} (\hat{a}^\dagger - \hat{a})$. A direct calculation gives

$$\langle \Psi_+, \hat{\alpha} \Psi_+ \rangle(\beta_+) = \sum_{n=0}^{\infty} \sqrt{2\hbar(n+1)} \operatorname{Re} (\bar{c}_n c_{n+1} \exp(-i\beta_+(\lambda_{n+1} - \lambda_n)/\hbar)) \quad (19)$$

$$\langle \Psi_+, \hat{p}_\alpha \Psi_+ \rangle(\beta_+) = \sum_{n=0}^{\infty} \sqrt{2\hbar(n+1)} \operatorname{Im} (\bar{c}_n c_{n+1} \exp(-i\beta_+(\lambda_{n+1} - \lambda_n)/\hbar)) \quad (20)$$

and similarly for moments.

Physical Hilbert spaces can be constructed and physical states decomposed in this way whenever one knows an explicit diagonalization of the Hamiltonian \hat{H} . For our model, the closeness to the harmonic oscillator has an additional advantage in that it allows us to use its simple form of coherent states — Gaussians of arbitrary width expanded in the stationary states — as initial values for evolution in β_+ . For the non-relativistic harmonic oscillator, the resulting physical states would be dynamical coherent states: their shape would remain unchanged and they keep saturating the uncertainty relation at all times. Moreover, their expectation values follow the classical trajectories exactly, without quantum back-reaction.

For the relativistic harmonic oscillator, and thus our anisotropic toy model, the dynamical behavior of the states is still to be seen. We thus assume an initial state, at some fixed value of β_+ , of the kinematical coherent form:

$$c_n = \exp\left(-\frac{|z|^2}{2}\right) \frac{z^n}{\sqrt{n!}} \quad , \quad z \in \mathbb{C} \quad (21)$$

such that $\Psi(\alpha, 0) = (2/\pi)^{1/4} \exp(-\frac{1}{2}(|z|^2 - z^2 + 2\alpha^2 - 4iz\alpha))$ from (16). A time-dependent physical state then has coefficients

$$c_n e^{-i\lambda_n \beta_+ / \hbar} = \frac{1}{\sqrt{n!}} e^{-|z|^2/2} z^n e^{-i\sqrt{2n+1}\beta_+ / \sqrt{\hbar}}$$

in its expansion by the $\varphi_n(\alpha)$. With the square root of $2n+1$, the exponentials cannot simply be combined to a β_+ -dependent $z(\beta_+)^n$. The shape of the state changes as β_+ moves away from zero: the time-dependent coefficients are no longer of the form (21) for $\beta_+ \neq 0$. Physical states with initial conditions given by the coherent states of the non-relativistic harmonic oscillator are not dynamical coherent states. The model introduced here does show spreading and quantum back-reaction, which makes it interesting for a comparison with effective constraint techniques.

2.3 Effective constraints

In an effective treatment of a quantum system, we can consider the same dynamics, but focus on the algebra of observables. Results will thus be manifestly representation independent. To set up this framework, no approximations are required; we are thus dealing with an exact quantum theory. Only when evaluating the equations, which would give us expressions such as $\langle \hat{\alpha} \rangle(\beta_+)$ or moments of a state as functions of β_+ , do approximation schemes typically enter. This is no difference to a representation dependent treatment, where exact evaluations of expectation values such as (19) or (20) are hard to sum explicitly.

At the kinematical level, effective techniques are based entirely on the algebra of basic operators, in our case $[\hat{\beta}_+, \hat{p}_+] = i\hbar$ and $[\hat{\alpha}, \hat{p}_\alpha] = i\hbar$, with all other basic commutators vanishing. As it happens at the quantum level, dynamics is brought in by a constraint operator \hat{C} which might have more complicated algebraic relationships with the basic operators, no longer forming a closed algebra.

A whole representation of these algebraic relationships on wave functions carries much more details than necessary for extracting physical results. Instead, it is often convenient to focus directly on expectation values and derive dynamical equations for them, avoiding the detour of computing wave functions. Expectation values are not sufficient to characterize a state or its dynamics, but when combined with all moments

$$\Delta(O_1 \dots O_n) := \left\langle \prod_{i=1}^n (\hat{O}_i - \langle \hat{O}_i \rangle) \right\rangle_{\text{Weyl}} \quad (22)$$

a complete set of variables results. Here, the subscript ‘‘Weyl’’ in the definition of the moments indicates that we are ordering all operator products totally symmetrically. Any of the basic operators, $\hat{\beta}_+$, \hat{p}_+ , $\hat{\alpha}$ and \hat{p}_α , can appear as the \hat{O}_i in the basic moments. (To match with standard notation, we will write $\Delta(O^2) = (\Delta O)^2$ for fluctuations.)

Expectation values of basic operators together with the moments can be used to characterize an arbitrary state (pure or mixed); they can be used as coordinates on the state space. Moreover, the commutator of basic operators endows the state space with a Poisson structure, defined by

$$\{\langle \hat{A} \rangle, \langle \hat{B} \rangle\} := \frac{\langle [\hat{A}, \hat{B}] \rangle}{i\hbar} \quad (23)$$

for any operators \hat{A} and \hat{B} . By linearity and the Leibniz rule, this defines Poisson brackets between all the moments and expectation values. In this way, the quantum phase space is defined. It is not a linear space since there are restrictions for the moments, most importantly the uncertainty relations such as

$$(\Delta\alpha)^2(\Delta p_\alpha)^2 - (\Delta(\alpha p_\alpha))^2 \geq \frac{\hbar^2}{4}. \quad (24)$$

On this kinematical quantum phase space, the constraint \hat{C} must be imposed. For a constraint operator polynomial in the basic operators,

$$C_{\text{pol}} := \langle (\widehat{\text{pol}} - \langle \widehat{\text{pol}} \rangle) \hat{C} \rangle \quad (25)$$

defines a function on the state space, expandable in the moments, for any arbitrary polynomial $\widehat{\text{pol}}$ of the basic operators. This infinite set of functions⁴ satisfies two important properties: (i) all these functions vanish on physical states annihilated by \hat{C} , and (ii) they form a first class set in the sense of classical constraint analysis, i.e. $\{C_{\text{pol}}, C_{\text{pol}'}\}$ vanishes on the subset of the phase space where all C_{pol} vanish. The quantum constraint \hat{C} can thus be implemented on the space of moments by imposing the infinite set $\{C_{\text{pol}}\}$ as constraints as one would do it on a classical phase space. We have to find the submanifold on which all constraints vanish, and factor out the flow generated by them. If this reduction is completed, we obtain the physical quantum phase space and can look for solutions of observables.

This procedure has several advantages [6]. As already mentioned, it is completely representation independent and instead focuses on algebraic aspects of a quantum system. As a consequence, implementing constraint operators with zero in their continuous spectra is no different from implementing those with zero in their discrete spectrum. Any difficulties in finding physical inner products can be avoided, for the physical normalization arises automatically when the constraints are solved for moments.

Once we try to find specific solutions, there are of course practical difficulties. We are dealing with infinitely many constraints on an infinite-dimensional phase space. Sometimes, this set of equations decouples to finitely many ones, but this happens only in rare solvable cases. In more general systems, we must use approximations to reduce the set to a finite one of relevant equations, with a semiclassical approximation as the main example. Here, we look for solutions whose moments satisfy a certain hierarchy, higher moments in the semiclassical case being suppressed by powers of \hbar , $\Delta(O_1 \dots O_n) \propto \hbar^{n/2}$. To any given order in \hbar , only a finite number of moments need be considered, subject to a finite number of non-trivial constraints.

In our model, to second order in moments we have the effective constraints

$$C = \langle \hat{p}_+ \rangle^2 - \langle \hat{p}_\alpha \rangle^2 - \langle \hat{\alpha} \rangle^2 + (\Delta p_+)^2 - (\Delta p_\alpha)^2 - (\Delta \alpha)^2 = 0 \quad (26)$$

$$C_{\beta_+} = 2\langle \hat{p}_+ \rangle \Delta(\beta_+ p_+) + i\hbar \langle \hat{p}_+ \rangle - 2\langle \hat{p}_\alpha \rangle \Delta(\beta_+ p_\alpha) - 2\langle \hat{\alpha} \rangle \Delta(\beta_+ \alpha) = 0 \quad (27)$$

$$C_{p_+} = 2\langle \hat{p}_+ \rangle (\Delta p_+)^2 - 2\langle \hat{p}_\alpha \rangle \Delta(p_+ p_\alpha) - 2\langle \hat{\alpha} \rangle \Delta(p_+ \alpha) = 0 \quad (28)$$

$$C_\alpha = 2\langle \hat{p}_+ \rangle \Delta(p_+ \alpha) - 2\langle \hat{p}_\alpha \rangle \Delta(\alpha p_\alpha) - i\hbar \langle \hat{p}_\alpha \rangle - 2\langle \hat{\alpha} \rangle (\Delta \alpha)^2 = 0 \quad (29)$$

$$C_{p_\alpha} = 2\langle \hat{p}_+ \rangle \Delta(p_+ p_\alpha) - 2\langle \hat{p}_\alpha \rangle (\Delta p_\alpha)^2 - 2\langle \hat{\alpha} \rangle \Delta(\alpha p_\alpha) + i\hbar \langle \hat{\alpha} \rangle = 0. \quad (30)$$

The reduction has been performed in [7], with the result that the physical state space is equivalent to a deparametrized quantum system with constraint $C_Q = \langle \hat{p}_+ \rangle \pm H_Q$ with the reduced Hamiltonian

$$H_Q = \sqrt{\langle \hat{p}_\alpha \rangle^2 + \langle \hat{\alpha} \rangle^2} \left(1 + \frac{\langle \hat{\alpha} \rangle^2 (\Delta p_\alpha)^2 - 2\langle \hat{\alpha} \rangle \langle \hat{p}_\alpha \rangle \Delta(\alpha p_\alpha) + \langle \hat{p}_\alpha \rangle^2 (\Delta \alpha)^2}{2(\langle \hat{p}_\alpha \rangle^2 + \langle \hat{\alpha} \rangle^2)^2} \right) \quad (31)$$

$$+ O((\Delta p_\alpha)^4) + O((\Delta \alpha)^4) + O((\Delta(\alpha p_\alpha))^2). \quad (32)$$

⁴A similar setup can be used in BRST quantizations, where the BRST charge would replace the constraint operators [10].

To leading order, we reproduce the classical Hamiltonian, but there are corrections from quantum fluctuations and correlations coupling to the expectation values. Moreover, from the Poisson brackets between moments we obtain Hamiltonian equations of motion telling us how a state spreads or is being squeezed. We have

$$\frac{d\langle\hat{\alpha}\rangle}{d\beta_+} = \frac{\langle\hat{p}_\alpha\rangle}{\sqrt{\langle\hat{p}_\alpha\rangle^2 + \langle\hat{\alpha}\rangle^2}} + \frac{\langle\hat{p}_\alpha\rangle(\Delta\alpha)^2(2\langle\hat{\alpha}\rangle^2 - \langle\hat{p}_\alpha\rangle^2) + \langle\hat{\alpha}\rangle\Delta(\alpha p_\alpha)(4\langle\hat{p}_\alpha\rangle^2 - 2\langle\hat{\alpha}\rangle^2) - 3\langle\hat{p}_\alpha\rangle\langle\hat{\alpha}\rangle^2(\Delta p_\alpha)^2}{2(\langle\hat{p}_\alpha\rangle^2 + \langle\hat{\alpha}\rangle^2)^{\frac{5}{2}}} \quad (33)$$

$$\frac{d\langle\hat{p}_\alpha\rangle}{d\beta_+} = \frac{-\langle\hat{\alpha}\rangle}{\sqrt{\langle\hat{p}_\alpha\rangle^2 + \langle\hat{\alpha}\rangle^2}} + \frac{3\langle\hat{\alpha}\rangle\langle\hat{p}_\alpha\rangle^2(\Delta\alpha)^2 - \langle\hat{p}_\alpha\rangle\Delta(\alpha p_\alpha)(4\langle\hat{\alpha}\rangle^2 - 2\langle\hat{p}_\alpha\rangle^2) - \langle\hat{\alpha}\rangle(\Delta p_\alpha)^2(2\langle\hat{p}_\alpha\rangle^2 - \langle\hat{\alpha}\rangle^2)}{2(\langle\hat{p}_\alpha\rangle^2 + \langle\hat{\alpha}\rangle^2)^{\frac{5}{2}}} \quad (34)$$

$$\frac{d(\Delta\alpha)^2}{d\beta_+} = \frac{2\langle\hat{\alpha}\rangle^2\Delta(\alpha p_\alpha) - 2\langle\hat{\alpha}\rangle\langle\hat{p}_\alpha\rangle(\Delta\alpha)^2}{(\langle\hat{p}_\alpha\rangle^2 + \langle\hat{\alpha}\rangle^2)^{\frac{3}{2}}} \quad (35)$$

$$\frac{d(\Delta p_\alpha)^2}{d\beta_+} = \frac{2\langle\hat{\alpha}\rangle\langle\hat{p}_\alpha\rangle(\Delta p_\alpha)^2 - 2\langle\hat{\alpha}\rangle^2\Delta(\alpha p_\alpha)}{(\langle\hat{p}_\alpha\rangle^2 + \langle\hat{\alpha}\rangle^2)^{\frac{3}{2}}} \quad (36)$$

$$\frac{d\Delta(\alpha p_\alpha)}{d\beta_+} = \frac{\langle\hat{\alpha}\rangle^2(\Delta p_\alpha)^2 - \langle\hat{p}_\alpha\rangle^2(\Delta\alpha)^2}{(\langle\hat{p}_\alpha\rangle^2 + \langle\hat{\alpha}\rangle^2)^{\frac{3}{2}}}. \quad (37)$$

Solutions $\langle\hat{\alpha}\rangle(\beta_+)$, $\langle\hat{p}_\alpha\rangle(\beta_+)$, $(\Delta\alpha)^2(\beta_+)$, $(\Delta p_\alpha)^2(\beta_+)$ and $\Delta(\alpha p_\alpha)(\beta_+)$ provide physical observables, corresponding to expectation values and moments in physical states, telling us how a state moves and spreads.

3 Comparison

Initially, the kinematical coherent state with expansion coefficients given by (21) yields the expectation values $\langle\hat{\alpha}\rangle|_{t=0} = \text{Re}(z)$ and $\langle\hat{p}_\alpha\rangle|_{t=0} = \text{Im}(z)$. The second order moments then saturate the uncertainty relation and their values are

$$(\Delta\alpha)^2|_{t=0} = \frac{\hbar}{2}, \quad (\Delta p_\alpha)^2|_{t=0} = \frac{\hbar}{2}, \quad \Delta(\alpha p_\alpha)|_{t=0} = 0.$$

For a concrete comparison we select a state that is initially peaked about $\langle\hat{\alpha}\rangle = \alpha_0$ and $\langle\hat{p}_\alpha\rangle = 0$, so that $z = \alpha_0$. In order for the state to be semiclassical, we need α_0 to be “significantly larger” than $\sqrt{\hbar}$. We make a concrete choice $\alpha_0 = 10\hbar^{\frac{1}{2}}$. In Fig. 1 we plot alongside each other the classical and two quantum-corrected trajectories of the system starting from the above initial values. The two corrected trajectories were calculated using two different methods: the kinematical coherent state of Section 2.2 and effective equations truncated at order \hbar , Eqs. (33)–(37) of Section 2.3.

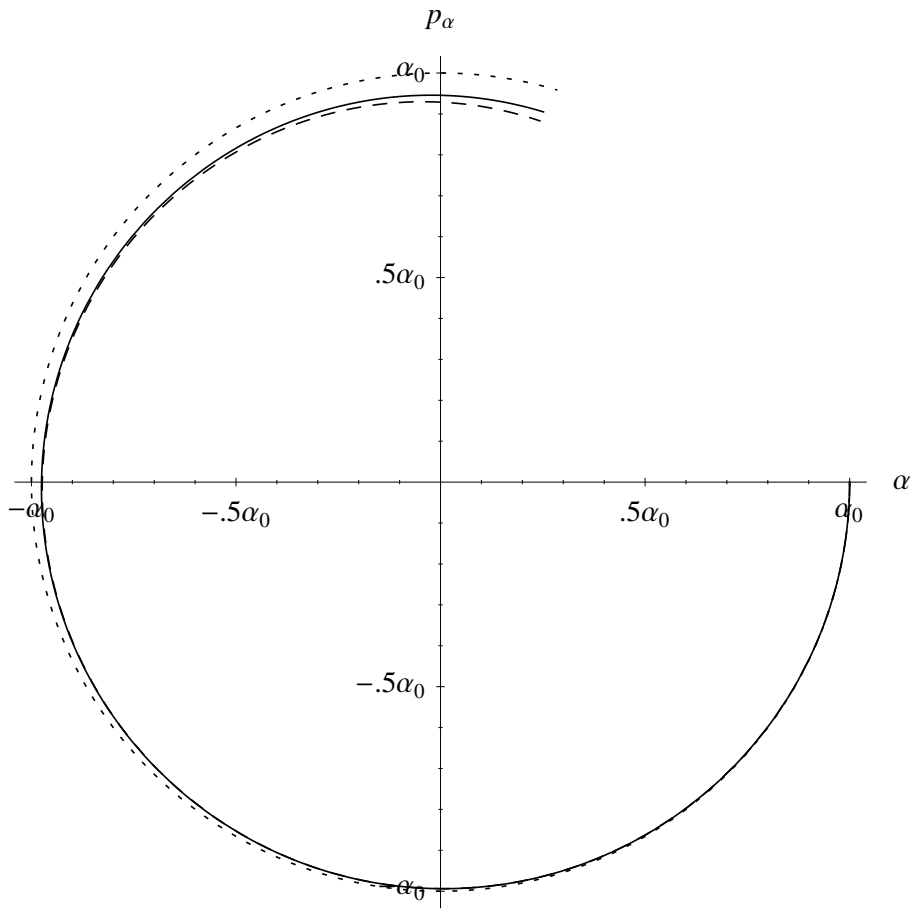


Figure 1: Classical (dotted), coherent state (solid) and effective (dashed) phase space trajectories, evolved for $0 \leq \beta_+ \leq 5\alpha_0$.

The two quantum trajectories agree very well for much of the evolution shown. In Figs. 2–4 we plot the quantum evolution of the second order moments generated by $\hat{\alpha}$ and \hat{p}_α . From Fig. 3 in particular it is clear that the semiclassical approximation breaks down somewhere between $\beta_+ = 2\alpha_0$ and $\beta_+ = 3\alpha_0$ as Δp_α is no longer “much smaller” than α_0 . Up until that point both methods for quantum evolution are in close agreement in describing not only the trajectory in the $\alpha - p_\alpha$ space but also the evolution of the second order moments themselves. Since semiclassicality was used to obtain the truncated system of equations, there is no reason to expect it to be accurate beyond $\beta_+ = 3\alpha_0$.

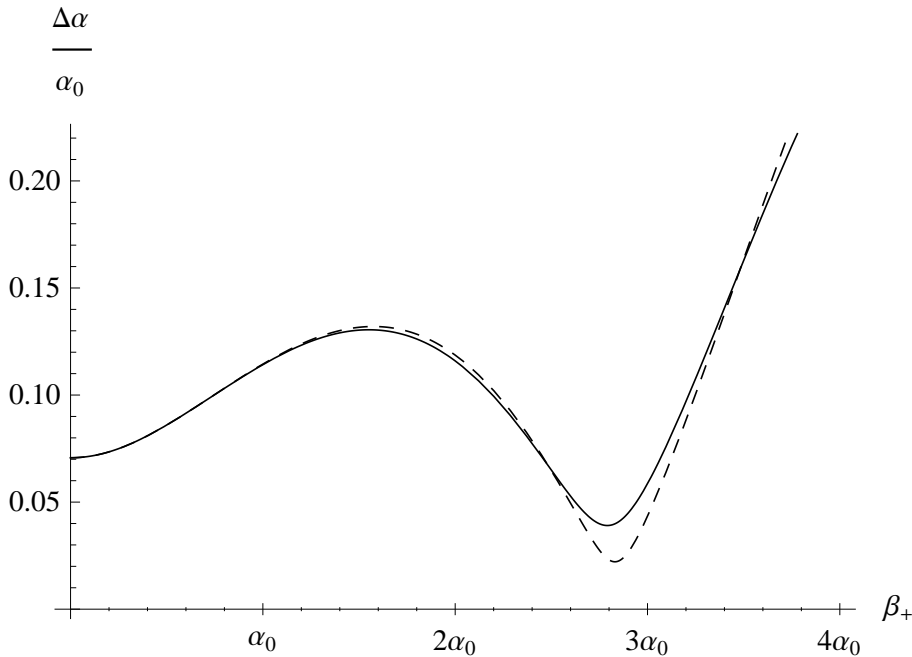


Figure 2: Coherent state (solid) and effective (dashed) evolution of the second order moment $\Delta\alpha = \sqrt{(\Delta\alpha)^2}$ in units of α_0 .

The two methods agree excellently where the domains of their applicability overlap. Both methods have their own strengths and weaknesses. The weakness of the semiclassically truncated effective equations should by now stand out — in some systems semiclassicality eventually breaks down and moments of high order dominate. Direct evaluation

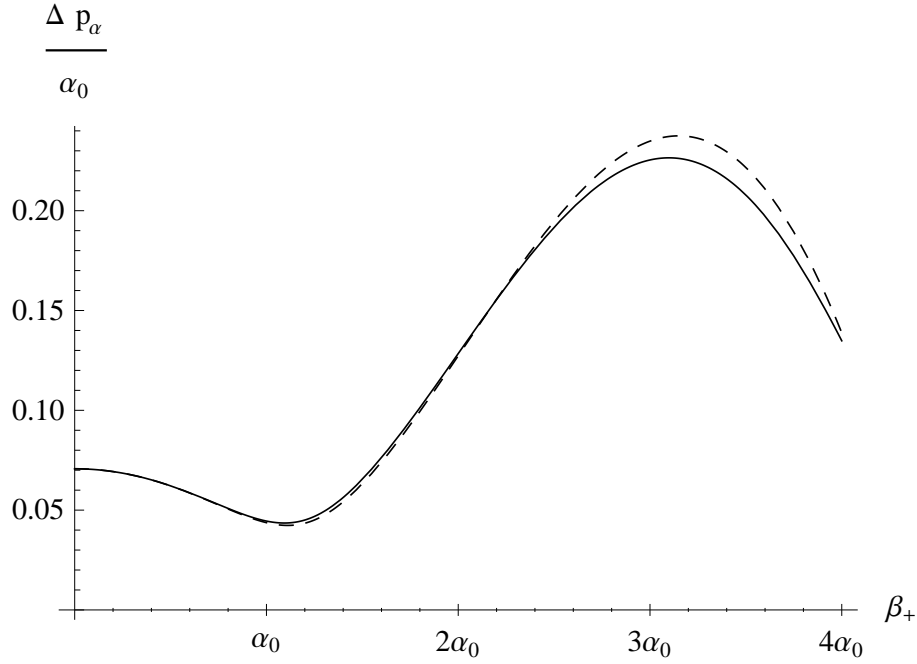


Figure 3: Coherent state (solid) and effective (dashed) evolution of the second order moment $\Delta p_\alpha = \sqrt{(\Delta p_\alpha)^2}$ in units of q_0 .

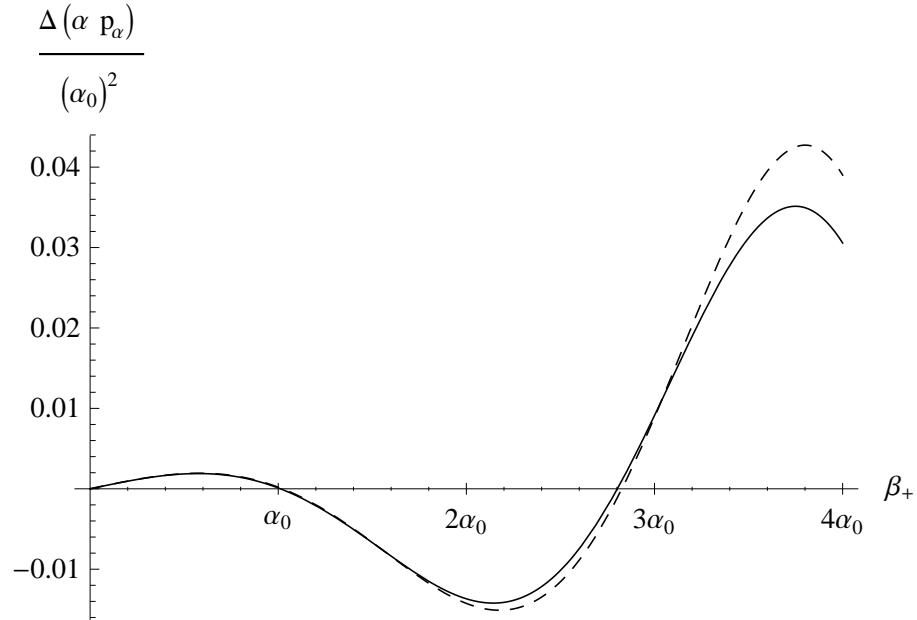


Figure 4: Coherent state (solid) and effective (dashed) evolution of the second order moment $\Delta(\alpha p_\alpha)$ in units of α_0^2 .

on the states does not rely on this approximation and remains a valid method for computing the wave function at all times. The shortcomings of the latter technique are less obvious and are of practical nature. In order to apply the method one needs, first of all, to decompose the initial state as a sum of the eigenstates of the Hamiltonian, which for an arbitrary state and a typical Hamiltonian can be complicated. During evolution, each of the eigenstates acquires a phase factor and they need to be re-summed to compute the wave function at a later time. For an arbitrary state, the sum may converge very slowly requiring one to sum over a very large number of eigenstates to obtain an accurate description of the wave function. Finally, for expectation values and moments of observables further integrations must be done. In systems of several degrees of freedom, this will add considerably to computation times.

If one is to make robust predictions, a range of initially semiclassical states with a variety of initial values of moments should be considered — the procedure is very complicated to implement using state decomposition but amounts to nothing more than simply changing the initial conditions in the case of the effective equations. In the subsections that follow we use the methods separately and exploit their individual strengths.

3.1 Long-term behavior of the state

Knowing the state exactly, allows us to plot the magnitude of the wave function and make precise long-term predictions. From Fig. 5 we see that after $\beta_+ \approx 10\alpha_0$ the state becomes highly quantum, spread out over an entire orbit. Expectation values can no longer be interpreted as the most probable outcome of a measurement.

In Figs. 6–8 we look at the long term behavior of the leading order quantum degrees of freedom. The magnitudes of $(\Delta\alpha)^2$ and $(\Delta p_\alpha)^2$ rise rapidly until around $\beta_+ = 40\alpha_0$. The state remains stable during $40\alpha_0 < \beta_+ < 200\alpha_0$ after which all second order moments begin to oscillate with an increasing amplitude. The amplitude reaches its peak around $\beta_+ = 300\alpha_0$; thereafter the moments keep oscillating with a stable amplitude for as long as the evolution has been traced, up to around $\beta_+ = 10^5\alpha_0$. As can be seen from the example of $\langle(\hat{\alpha} - \langle\hat{\alpha}\rangle)^3\rangle$ in Fig. 9, third order moments follow a similar pattern.

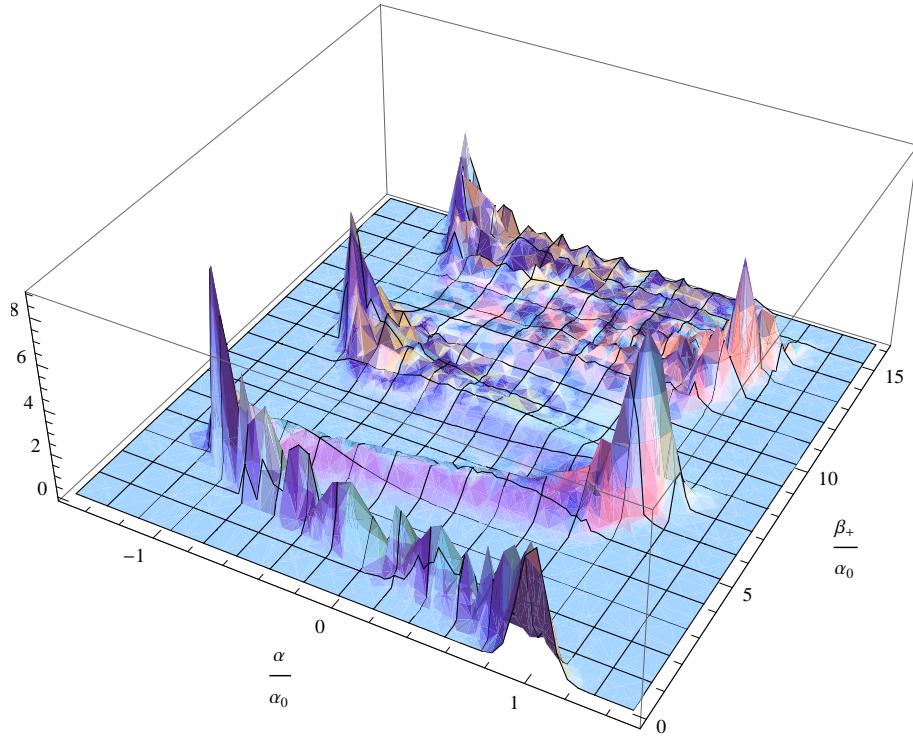


Figure 5: Square-magnitude of the coherent state wave function evolved for $0 < \beta_+ < 15\alpha_0$.

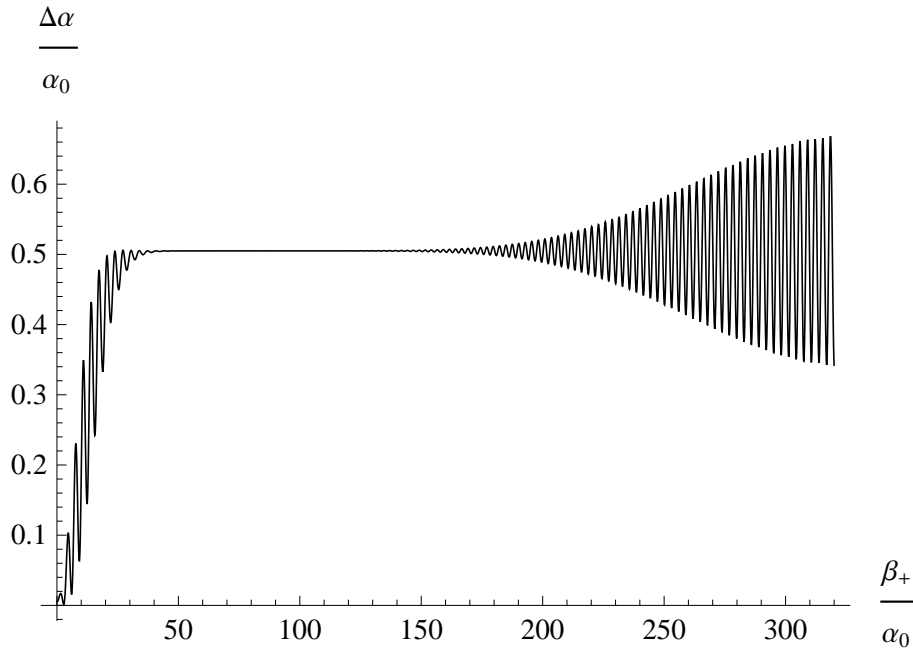


Figure 6: Coherent state evolution of the second order moment $\Delta\alpha = \sqrt{(\Delta\alpha)^2}$ in units of α_0 .

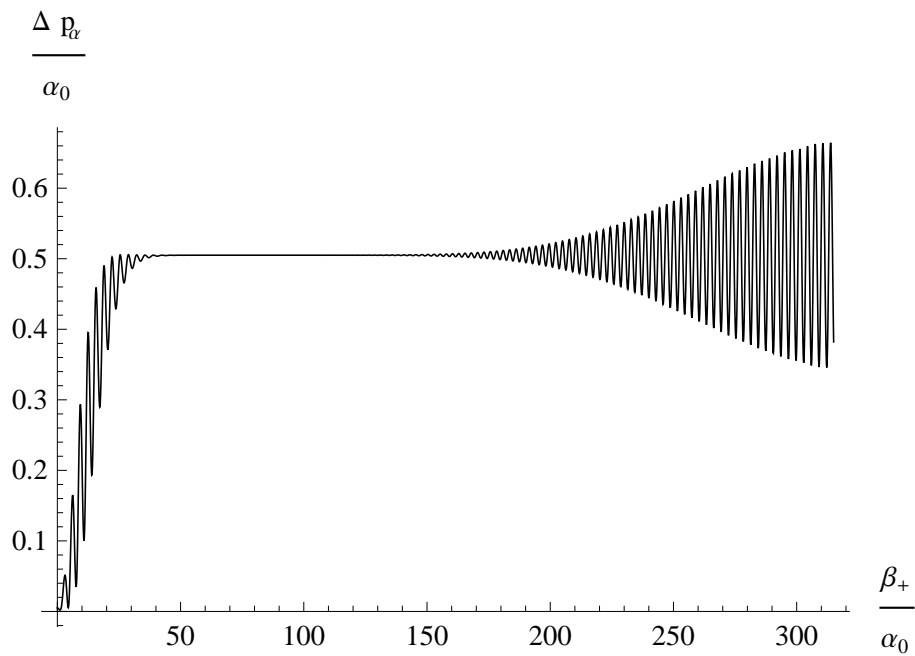


Figure 7: Coherent state (solid) and effective (dashed) evolution of the second order moment $\Delta p_\alpha = \sqrt{(\Delta p_\alpha)^2}$ in units of α_0 .

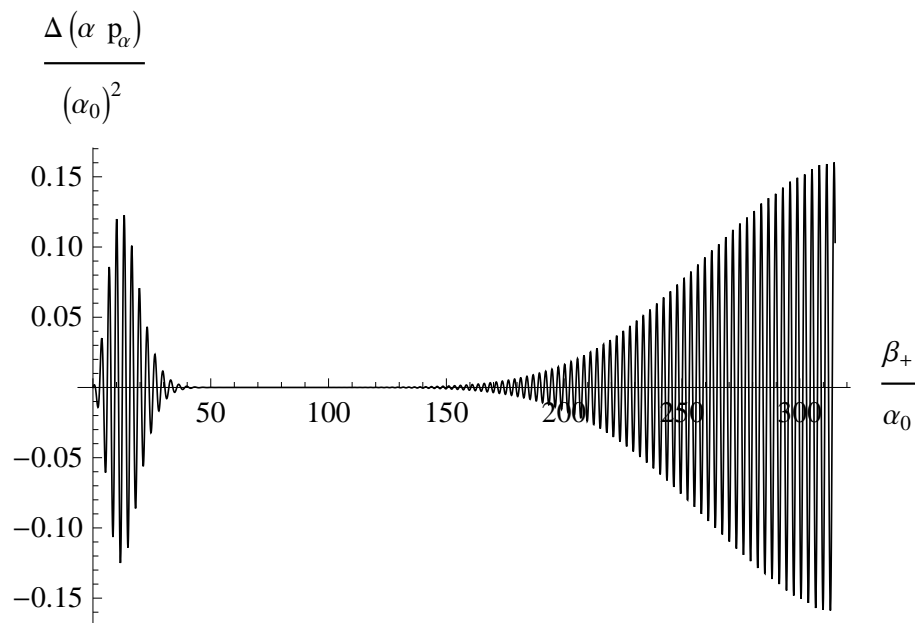


Figure 8: Coherent state (solid) and effective (dashed) evolution of the second order moment $\Delta(\alpha p_\alpha)$ in units of α_0 .

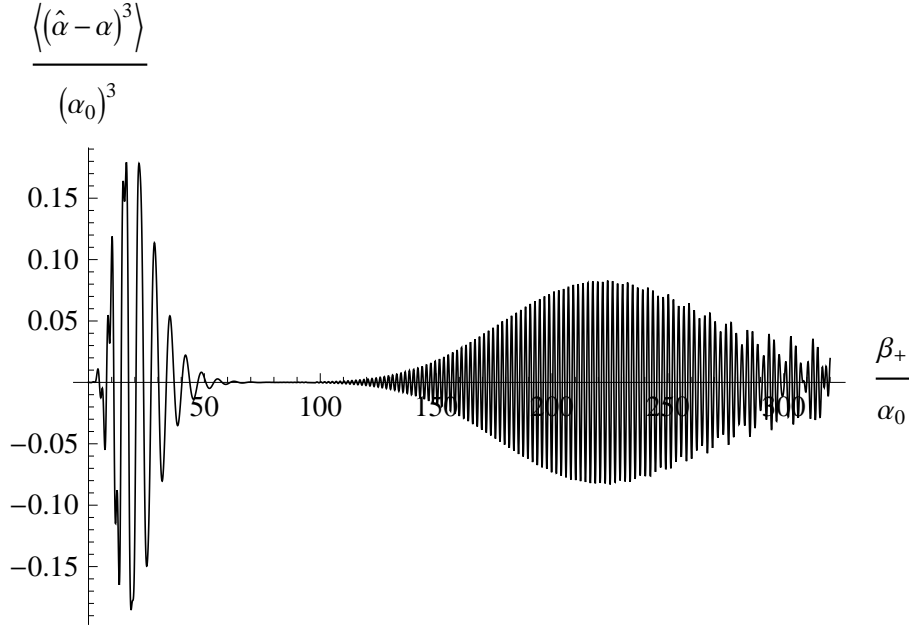


Figure 9: Coherent state evolution of the third order moment $\langle(\hat{\alpha} - \langle\hat{\alpha}\rangle)^3\rangle$ in units of α_0 .

As expected, semiclassicality eventually breaks down and quantum fluctuations become large; this trend is illustrated by the evolving uncertainty measure $(\Delta\alpha)^2(\Delta p_\alpha)^2 - (\Delta(\alpha p_\alpha))^2$ (bounded below by the uncertainty relation) shown in Fig. 10. After the initial increase, there is a period of approximate stability; then the leading order fluctuations start to oscillate with large amplitudes. Even though some moments return to small values during these oscillations, semiclassicality is not regained as shown by the long-term behavior of the uncertainties in Fig. 11. Details of this behavior, found numerically, appears rather characteristic, but it is difficult to find an explanation based on the underlying equations.

3.2 Short-term evolution with varying initial conditions

We now evolve effectively starting from the same initial expectation values, but varying the initial values of second order moments. By the specific choices, some sets of moments used here no longer saturate the uncertainty relations, and some have non-vanishing correlations. They cannot correspond to Gaussian states, and so their initial configurations would be much more difficult to implement using wave functions of physical states. The results are plotted in Fig. 12. In Figs. 13–16 we plot the corresponding effective evolution of moments for each set of the initial conditions, where the thin horizontal line approximately indicates the threshold of the semiclassical approximation for the second order moments at $.04\alpha_0^2$.

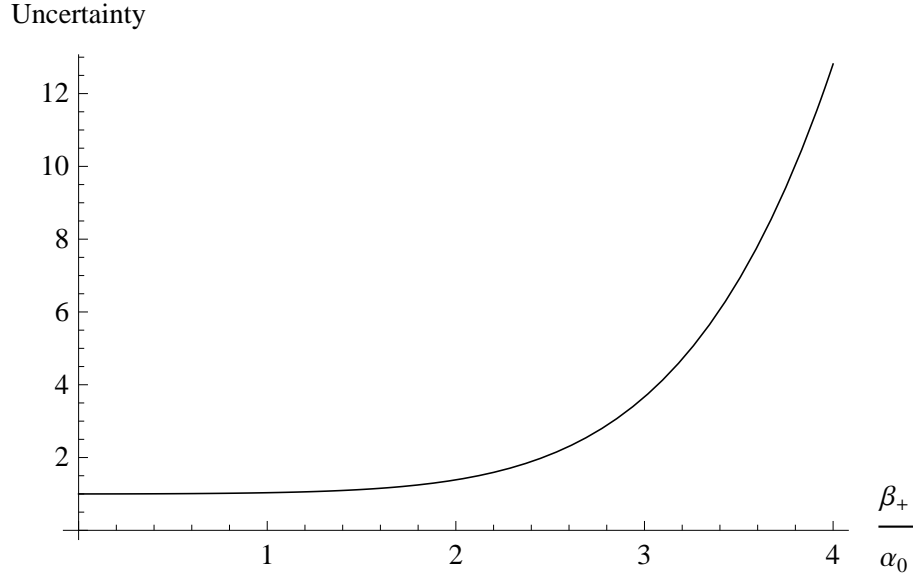


Figure 10: Short-term coherent state evolution of the “quantum uncertainty” defined as $(\Delta\alpha)^2(\Delta p_\alpha)^2 - (\Delta(\alpha p_\alpha))^2$ in units of $\frac{\hbar^2}{4}$.

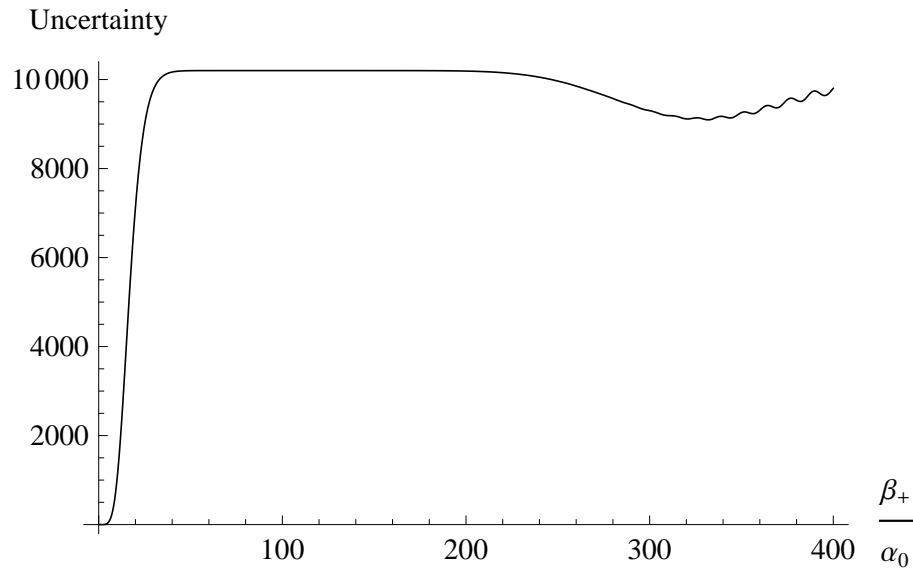


Figure 11: Long-term coherent state evolution of the “quantum uncertainty” defined as $(\Delta\alpha)^2(\Delta p_\alpha)^2 - (\Delta(\alpha p_\alpha))^2$ in units of $\frac{\hbar^2}{4}$.

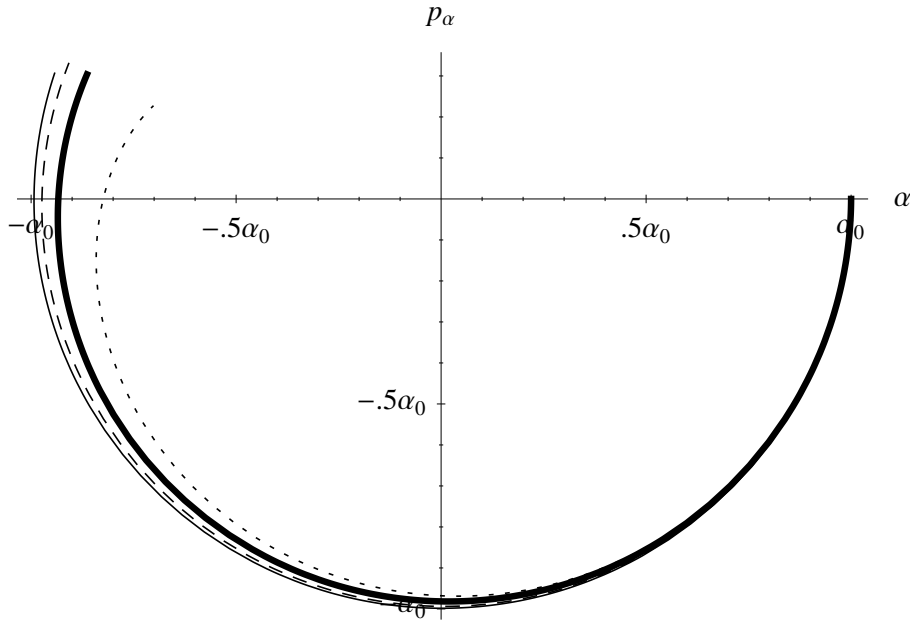


Figure 12: Effective evolution of semiclassical states with different initial values of moments for $0 < \beta_+ < 3.5\alpha_0$. The initial values of moments are as follows. Dashed line—the original coherent state: $(\Delta\alpha)^2 = (\Delta p_\alpha)^2 = .005\alpha_0^2$, $\Delta(\alpha p_\alpha) = 0$. Dotted line: $(\Delta\alpha)^2 = .025\alpha_0^2$, $(\Delta p_\alpha)^2 = .001\alpha_0^2$, $\Delta(\alpha p_\alpha) = 0$. Thin solid line: $(\Delta\alpha)^2 = .001\alpha_0^2$, $(\Delta p_\alpha)^2 = .025\alpha_0^2$, $\Delta(\alpha p_\alpha) = 0$. Thick solid line: $(\Delta\alpha)^2 = .008\alpha_0^2$, $(\Delta p_\alpha)^2 = .008\alpha_0^2$, $\Delta(\alpha p_\alpha) = .005\alpha_0^2$.

Larger $(\Delta\alpha)^2$ results in a larger deviation from the classical behavior and a faster breakdown of the semiclassical approximation. The above effect is much less sensitive to the momentum spread $(\Delta p_\alpha)^2$. This disparity between the effects of the two spreads may seem surprising given the symmetry between $\hat{\alpha}$ and \hat{p}_α in the expression for the physical Hamiltonian. This symmetry, however is broken by the initial state we have chosen, which is peaked about $\langle \hat{p}_\alpha \rangle = 0$ and $\langle \hat{\alpha} \rangle = \alpha_0$, so that the spread in α , produces a larger spread in the energy than the spread in p_α .

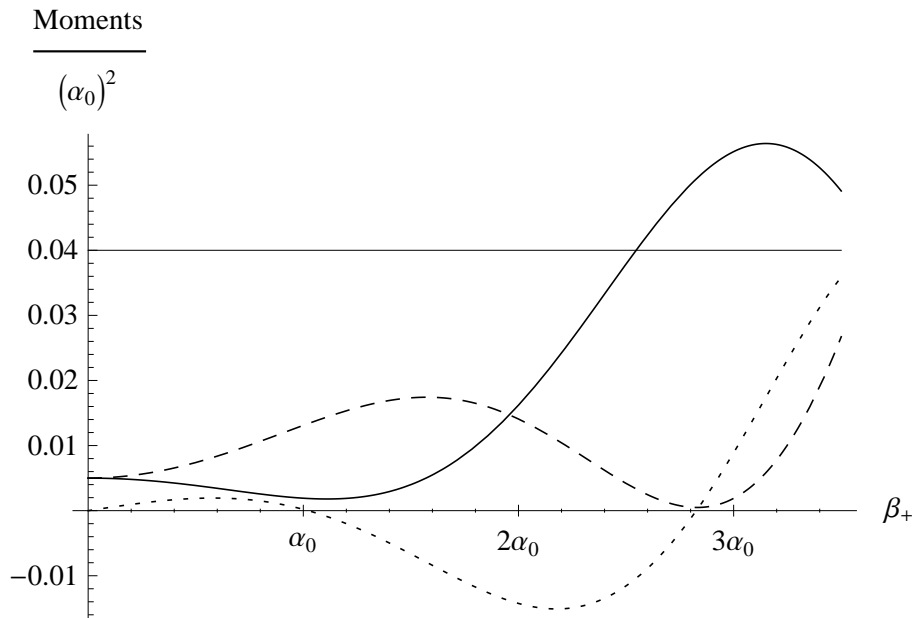


Figure 13: Effective evolution of second order moments $(\Delta\alpha)^2$ (dashed), $(\Delta p_\alpha)^2$ (solid) and $\Delta(\alpha p_\alpha)$ (dotted), which initially take the values $.005\alpha_0^2$, $.005\alpha_0^2$ and 0 respectively.

4 Effective evolution of a radiation-filled universe

In this section we use the effective equations on their own to analyze quantum corrections to the dynamics of a radiation-filled Bianchi I universe briefly mentioned in Section 2. This

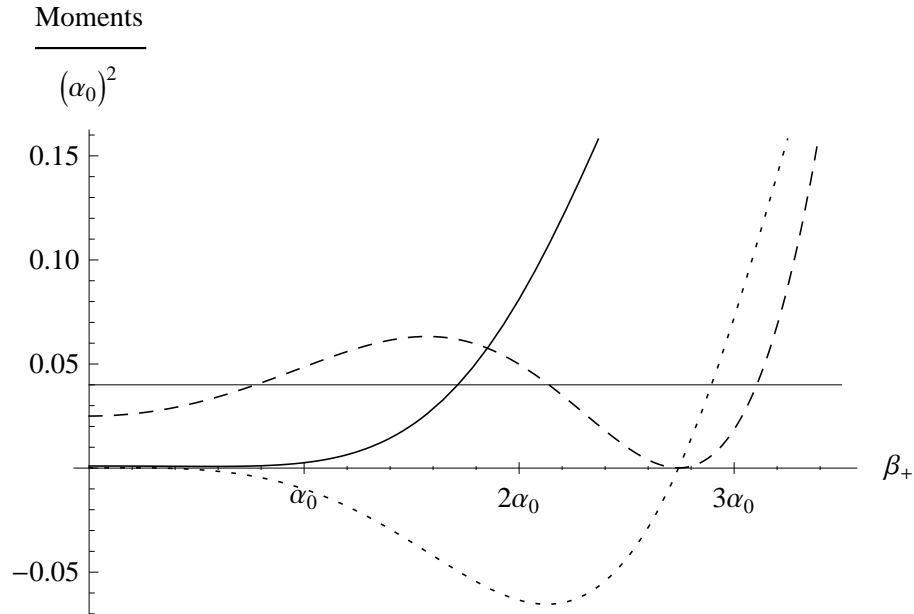


Figure 14: Effective evolution of second order moments $(\Delta\alpha)^2$ (dashed), $(\Delta p_\alpha)^2$ (solid) and $\Delta(\alpha p_\alpha)$ (dotted), which initially take the values $.025\alpha_0^2$, $.001\alpha_0^2$ and 0 respectively.

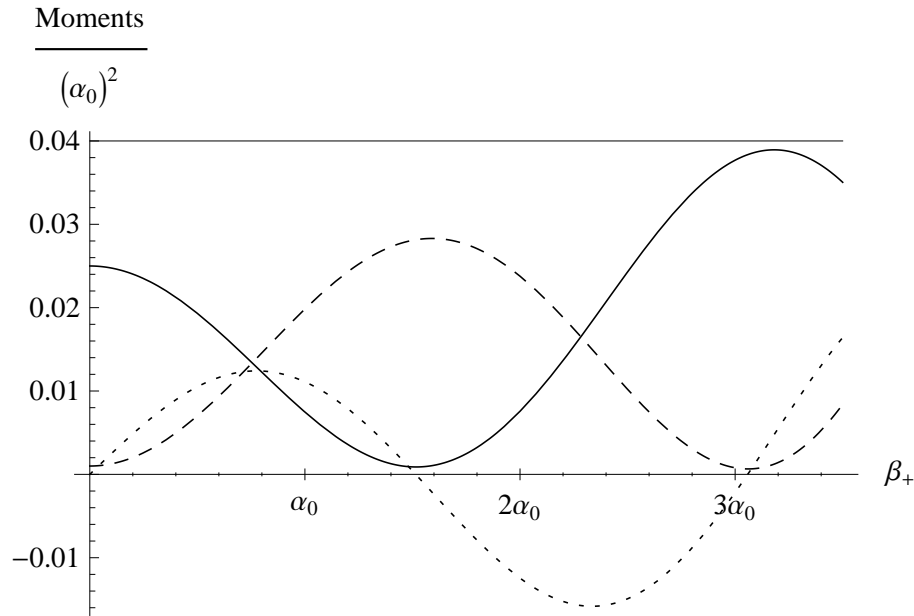


Figure 15: Effective evolution of second order moments $(\Delta\alpha)^2$ (dashed), $(\Delta p_\alpha)^2$ (solid) and $\Delta(\alpha p_\alpha)$ (dotted), which initially take the values $.001\alpha_0^2$, $.025\alpha_0^2$ and 0 respectively.

Moments

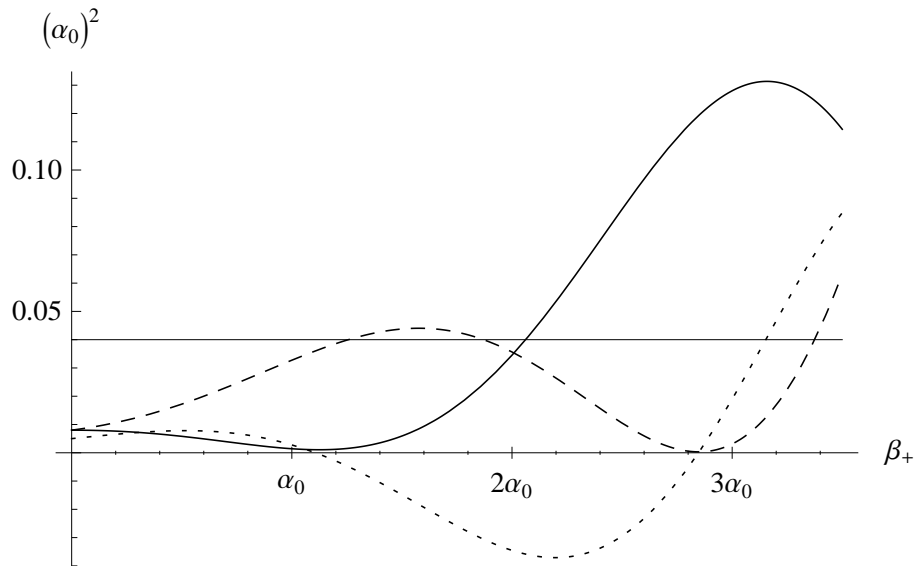


Figure 16: Effective evolution of second order moments $(\Delta\alpha)^2$ (dashed), $(\Delta p_\alpha)^2$ (solid) and $\Delta(\alpha p_\alpha)$ (dotted), which initially take the values $.008\alpha_0^2$, $.008\alpha_0^2$ and $.005\alpha_0^2$ respectively.

model has a more realistic matter content than the one analyzed above. We recall that the energy density of radiation has the form $\rho \propto a^{-4} = e^{-4\alpha}$, which results in the Hamiltonian constraint $C = p_+^2 - p_\alpha^2 + e^{2\alpha}\nu$. The constraint condition may be implemented effectively in fashion a very similar to the way it was done in Section 2.3; however, the physical inner product treatment would require a detailed knowledge of the (now continuous) spectrum of an operator that is completely different from \hat{H} that was used in (15) and is not straightforward to obtain. Even if we could determine energy eigenstates, expanding Gaussians or other general semiclassical states in this basis would be challenging. For this reason we do not attempt to implement the constraint of the radiation-filled model on the kinematical Hilbert space and restrict our analysis to the effective procedure, demonstrating its wide applicability.

4.1 Classical behavior

We deparametrize the constraint exactly as in Section 2.1, selecting β_+ as time. The dynamics on α and p_α is then generated by the Hamiltonian $H = \sqrt{p_\alpha^2 - e^{2\alpha}\nu}$ and results in the equations of motion $d\alpha/d\beta_+ = p_\alpha/H$ and $dp_\alpha/d\beta_+ = e^{2\alpha}\nu/H$. Noting that H is once again a constant of motion we can immediately infer the classical phase-space trajectories, which are of the form $p_\alpha = \pm\sqrt{e^{2\alpha}\nu + \text{const}}$. They split the $\alpha - p_\alpha$ space into three regions as illustrated in Fig. 17. There are no classical orbits in Region 3, as H becomes complex.

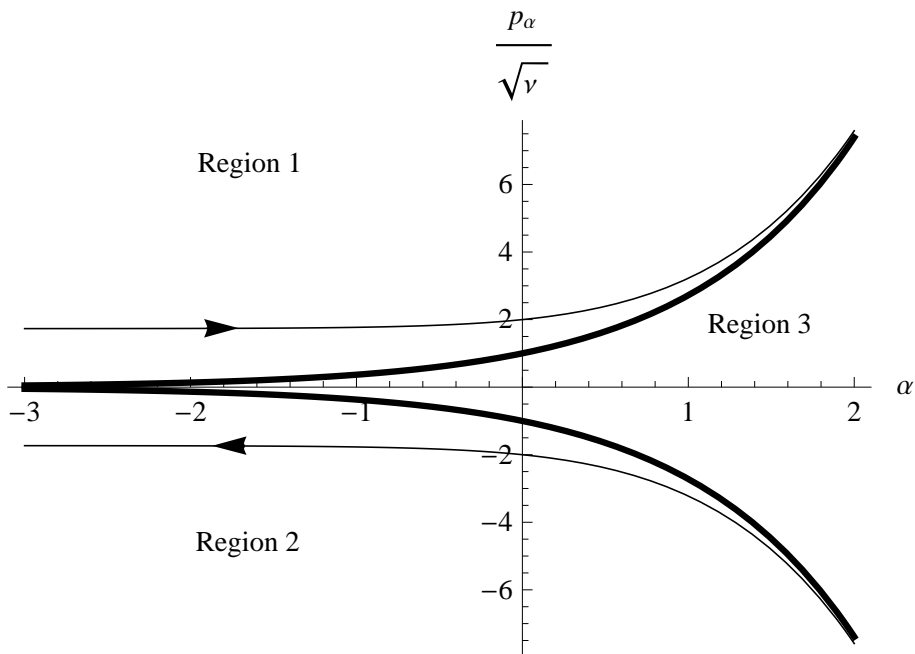


Figure 17: Disjoint regions of classical solutions. Region 1: trajectories have the shape $p_\alpha = \sqrt{e^{2\alpha\nu} + \text{const}}$, they correspond to expanding universes as α increases with β_+ . Region 2: trajectories have the shape $p_\alpha = -\sqrt{e^{2\alpha\nu} + \text{const}}$, they correspond to contracting universes as α decreases with β_+ . Region 3: no classical solutions.

The explicit solution to the equations of motion for evolution in terms of β_+ is given by

$$\alpha(\beta_+) = \beta_+ - \log(2(1 + Ae^{2\beta_+})) + B \quad (38)$$

where the integration constants A and B can be related to the initial values $\alpha_0 := \alpha(0)$ and $p_{\alpha 0} := p_\alpha(0)$ via

$$A = 1 + \frac{2p_{\alpha 0}}{e^{2\alpha_0}\nu} \left(\sqrt{p_{\alpha 0}^2 - e^{2\alpha_0}\nu} - p_{\alpha 0} \right)$$

$$B = \log \left(4 + \frac{4p_{\alpha 0}}{e^{2\alpha_0}\nu} \left(\sqrt{p_{\alpha 0}^2 - e^{2\alpha_0}\nu} - p_{\alpha 0} \right) \right) + \alpha_0$$

In terms of A and B , the constant of motion is

$$H^2 = \frac{-e^{2B}\nu}{16A}$$

which requires $A < 0$ in order for H to be real. Using (38), $p_\alpha(\beta_+)$ may be recovered from the equations of motion as $p_\alpha(\beta_+) = H d\alpha/d\beta_+$.

For the orbits in Region 1, α and p_α reach infinity at a finite positive value of the evolution parameter, namely at $\beta_+ = \alpha_0 - \log(p_{\alpha 0} - H)$. Explicit integration of the expression (11) for the proper time using the above solution for $\alpha(\beta_+)$ shows that this value of β_+ is reached in infinite proper time. In other words, the expansion, as expected for the radiation filled universe, takes infinite proper time, but anisotropy asymptotically approaches a maximum value. For the orbits in Region 2 one can obtain a similar result by tracing evolution backwards in time; in this case α reaches infinity and p_α reaches negative infinity at $\beta_+ = \alpha_0 - \log(|p_{\alpha 0}| + H)$, which is always negative in that region.

Following those orbits forward in time, one finds that the collapse happens only as β_+ goes to infinity. Once again one can use (11) to convert this to a proper time interval, with the result that, as one would expect, the collapse takes a finite amount of proper time,

$$\Delta\tau := \tau(\beta_+ = \infty) - \tau(\beta_+ = 0) = \frac{a_0^3 e^{2B}}{32\sqrt{|A|\nu}} \left(\frac{1 + |A|}{(|A| - 1)^2} - \frac{\cosh^{-1}(\sqrt{|A|})}{\sqrt{|A|}} \right).$$

In this model, with positive energy, the singularity is certainly not resolved.

4.2 Effective constraints

Following the effective procedure for solving constraints outlined in Section 2.3 we find the constraint functions truncated at second order:

$$C = \langle \hat{p}_+ \rangle^2 - \langle \hat{p}_\alpha \rangle^2 + e^{2\langle \hat{\alpha} \rangle} \nu + (\Delta p_+)^2 - (\Delta p_\alpha)^2 + 2e^{2\langle \hat{\alpha} \rangle} \nu (\Delta \alpha)^2 = 0 \quad (39)$$

$$C_{\beta_+} = 2\langle \hat{p}_+ \rangle \Delta(\beta_+ p_+) + i\hbar \langle \hat{p}_+ \rangle - 2\langle \hat{p}_\alpha \rangle \Delta(\beta_+ p_\alpha) + 2e^{2\langle \hat{\alpha} \rangle} \nu \Delta(\beta_+ \alpha) = 0 \quad (40)$$

$$C_{p_+} = 2\langle \hat{p}_+ \rangle (\Delta p_+)^2 - 2\langle \hat{p}_\alpha \rangle \Delta(p_+ p_\alpha) + 2e^{2\langle \hat{\alpha} \rangle} \nu \Delta(p_+ \alpha) = 0 \quad (41)$$

$$C_\alpha = 2\langle \hat{p}_+ \rangle \Delta(p_+ \alpha) - 2\langle \hat{p}_\alpha \rangle \Delta(\alpha p_\alpha) - i\hbar \langle \hat{p}_\alpha \rangle + 2e^{2\langle \hat{\alpha} \rangle} \nu (\Delta \alpha)^2 = 0 \quad (42)$$

$$C_{p_\alpha} = 2\langle \hat{p}_+ \rangle \Delta(p_+ p_\alpha) - 2\langle \hat{p}_\alpha \rangle (\Delta p_\alpha)^2 + 2e^{2\langle \hat{\alpha} \rangle} \nu \Delta(\alpha p_\alpha) - i\hbar e^{2\langle \hat{\alpha} \rangle} \nu = 0. \quad (43)$$

These can be solved and gauge fixed following the same steps as for the model of Section 2.3, with the result that evolution in β_+ on the expectation values and moments of $\hat{\alpha}$ and \hat{p}_α is generated by the quantum Hamiltonian

$$H_Q = \sqrt{\langle \hat{p}_\alpha \rangle^2 - e^{2\langle \hat{\alpha} \rangle} \nu} \left(1 + e^{2\langle \hat{\alpha} \rangle} \nu \frac{-(\Delta p_\alpha)^2 + 2\langle \hat{p}_\alpha \rangle \Delta(\alpha p_\alpha) + (e^{2\langle \hat{\alpha} \rangle} \nu - 2\langle \hat{p}_\alpha \rangle^2)(\Delta \alpha)^2}{2(\langle \hat{p}_\alpha \rangle^2 - e^{2\langle \hat{\alpha} \rangle} \nu)^2} \right) + O((\Delta p_\alpha)^4) + O((\Delta \alpha)^4) + O((\Delta(\alpha p_\alpha))^2). \quad (44)$$

The equations of motion are obtained by taking the quantum Poisson bracket between quantum variables and the quantum Hamiltonian.

$$\frac{d\langle \hat{\alpha} \rangle}{d\beta_+} = \frac{\langle \hat{p}_\alpha \rangle}{\sqrt{\langle \hat{p}_\alpha \rangle^2 - e^{2\langle \hat{\alpha} \rangle} \nu}} + e^{2\langle \hat{\alpha} \rangle} \nu \frac{\langle \hat{p}_\alpha \rangle (\langle \hat{p}_\alpha \rangle^2 + \frac{1}{2} e^{2\langle \hat{\alpha} \rangle} \nu) (\Delta \alpha)^2 - \Delta(\alpha p_\alpha) (2\langle \hat{p}_\alpha \rangle^2 + e^{2\langle \hat{\alpha} \rangle} \nu) - \frac{3}{2} \langle \hat{p}_\alpha \rangle (\Delta p_\alpha)^2}{2(\langle \hat{p}_\alpha \rangle^2 - e^{2\langle \hat{\alpha} \rangle} \nu)^{\frac{5}{2}}} \quad (45)$$

$$\frac{d\langle \hat{p}_\alpha \rangle}{d\beta_+} = \frac{-\langle \hat{\alpha} \rangle}{\sqrt{\langle \hat{p}_\alpha \rangle^2 - e^{2\langle \hat{\alpha} \rangle} \nu}} + e^{2\langle \hat{\alpha} \rangle} \nu \frac{(\frac{1}{2} e^{4\langle \hat{\alpha} \rangle} \nu^2 - \langle \hat{p}_\alpha \rangle^2 e^{2\langle \hat{\alpha} \rangle} \nu + 2\langle \hat{p}_\alpha \rangle^4)(\Delta \alpha)^2 - 2\Delta(\alpha p_\alpha) (\frac{1}{2} e^{2\langle \hat{\alpha} \rangle} \nu + \langle \hat{p}_\alpha \rangle^2) \langle \hat{p}_\alpha \rangle}{(\langle \hat{p}_\alpha \rangle^2 - e^{2\langle \hat{\alpha} \rangle} \nu)^{\frac{3}{2}}} + e^{2\langle \hat{\alpha} \rangle} \nu \frac{(\Delta p_\alpha)^2 (\langle \hat{p}_\alpha \rangle^2 + \frac{1}{2} e^{2\langle \hat{\alpha} \rangle} \nu)}{2(\langle \hat{p}_\alpha \rangle^2 - e^{2\langle \hat{\alpha} \rangle} \nu)^{\frac{5}{2}}} \quad (46)$$

$$\frac{d(\Delta \alpha)^2}{d\beta_+} = \frac{2e^{2\langle \hat{\alpha} \rangle} \nu (\langle \hat{p}_\alpha \rangle (\Delta \alpha)^2 - \Delta(\alpha p_\alpha))}{(\langle \hat{p}_\alpha \rangle^2 - e^{2\langle \hat{\alpha} \rangle} \nu)^{\frac{3}{2}}} \quad (47)$$

$$\frac{d(\Delta p_\alpha)^2}{d\beta_+} = \frac{2e^{2\langle \hat{\alpha} \rangle} \nu ((2\langle \hat{p}_\alpha \rangle^2 - e^{2\langle \hat{\alpha} \rangle} \nu) \Delta(\alpha p_\alpha) - \langle \hat{p}_\alpha \rangle (\Delta p_\alpha)^2)}{(\langle \hat{p}_\alpha \rangle^2 - e^{2\langle \hat{\alpha} \rangle} \nu)^{\frac{3}{2}}} \quad (48)$$

$$\frac{d\Delta(\alpha p_\alpha)}{d\beta_+} = \frac{e^{2\langle \hat{\alpha} \rangle} \nu ((2\langle \hat{p}_\alpha \rangle^2 - e^{2\langle \hat{\alpha} \rangle} \nu) (\Delta \alpha)^2 - (\Delta p_\alpha)^2)}{(\langle \hat{p}_\alpha \rangle^2 - e^{2\langle \hat{\alpha} \rangle} \nu)^{\frac{3}{2}}}. \quad (49)$$

As before, these equations reduce to the classical equations of motion at zeroth order in moments and are straightforward to evolve numerically.

4.3 Numerical evolution

In this section we take a classical phase space trajectory from each of the Regions 1 and 2 and compare the effective trajectories for a variety of semiclassical states initially peaked about these classical solutions. Effective and classical trajectories of the expanding universe are plotted in Fig. 18. Clearly, the significance of quantum back-reaction can be seen well before the approximation breaks down.

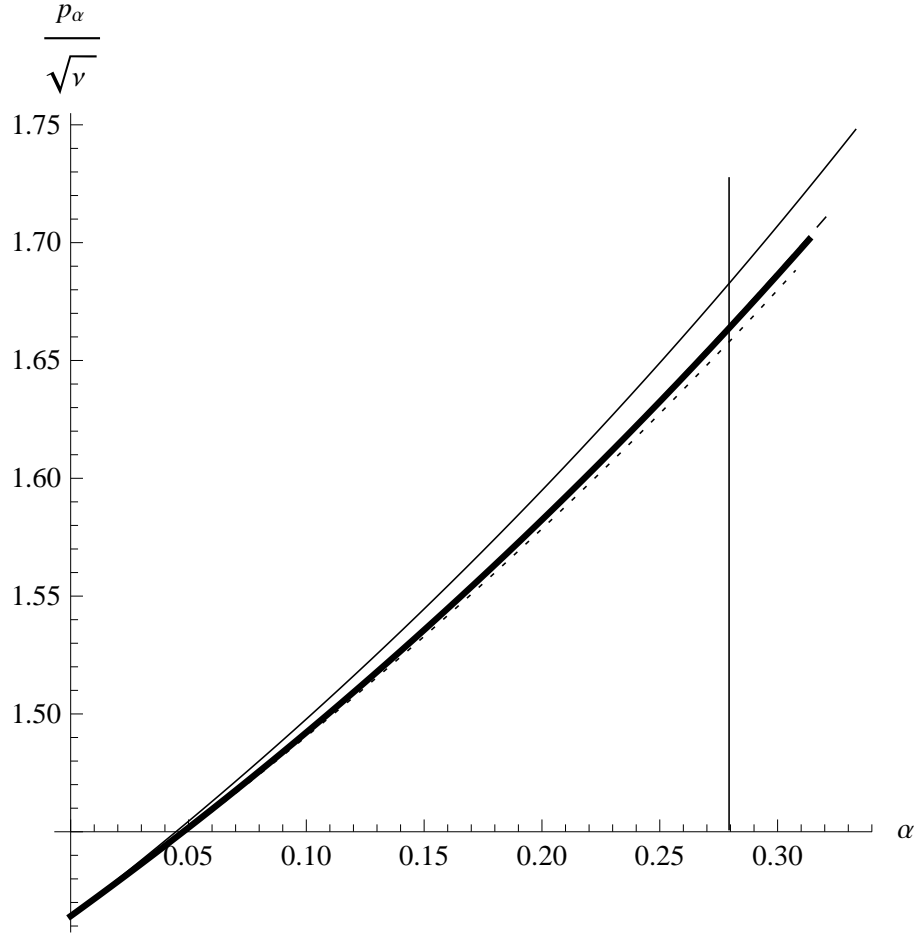


Figure 18: Phase space trajectories of an expanding universe classical (dotted) and effective with different initial values for second order moments: dashed line— $(\Delta\alpha)^2\nu = .001H_0^2$, $(\Delta p_\alpha)^2 = .025H_0^2$, $\Delta(\alpha p_\alpha)\sqrt{\nu} = 0$; thin solid line— $(\Delta\alpha)^2\nu = .025H_0^2$, $(\Delta p_\alpha)^2 = .001H_0^2$, $\Delta(\alpha p_\alpha)\sqrt{\nu} = 0$; thick solid line— $(\Delta\alpha)^2\nu = .008H_0^2$, $(\Delta p_\alpha)^2 = .008H_0^2$, $\Delta(\alpha p_\alpha)\sqrt{\nu} = .005H_0^2$. Solutions were evolved for $0 < \beta_+ < .2$; the vertical line indicates the breakdown of the semiclassical approximation based on the size of second order moments.

The corresponding evolution of the leading order moments starting from different initial values is plotted in Figs. 19-21, where the horizontal line, as before, indicates an approximate threshold of the semiclassical approximation for the second order moments.

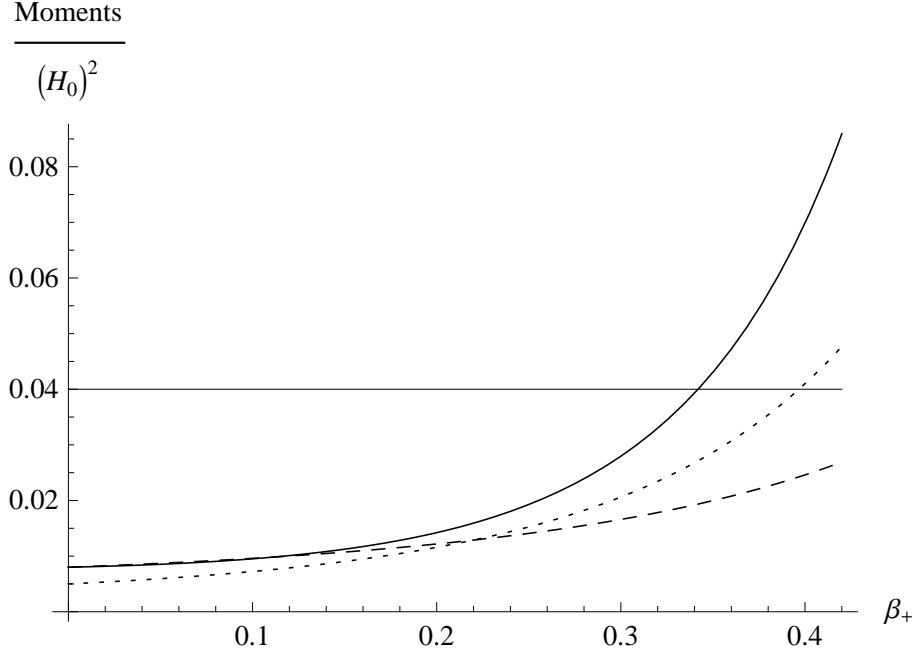


Figure 19: Evolution of second order moments in an expanding universe. $(\Delta\alpha)^2\nu$ (dashed), $(\Delta p_\alpha)^2$ (solid), $\Delta(\alpha p_\alpha)\sqrt{\nu}$ (dotted), with initial values: $(\Delta\alpha)^2\nu = .008H_0^2$, $(\Delta p_\alpha)^2 = .008H_0^2$, $\Delta(\alpha p_\alpha)\sqrt{\nu} = .005H_0^2$.

Effective and classical trajectories of the contracting universe are plotted in Fig. 22. The corresponding evolution of the leading order moments starting from different initial values is plotted in Figs. 23-25, where the horizontal line, once again, indicates an approximate threshold of the semiclassical approximation for the second order moments.

Moments

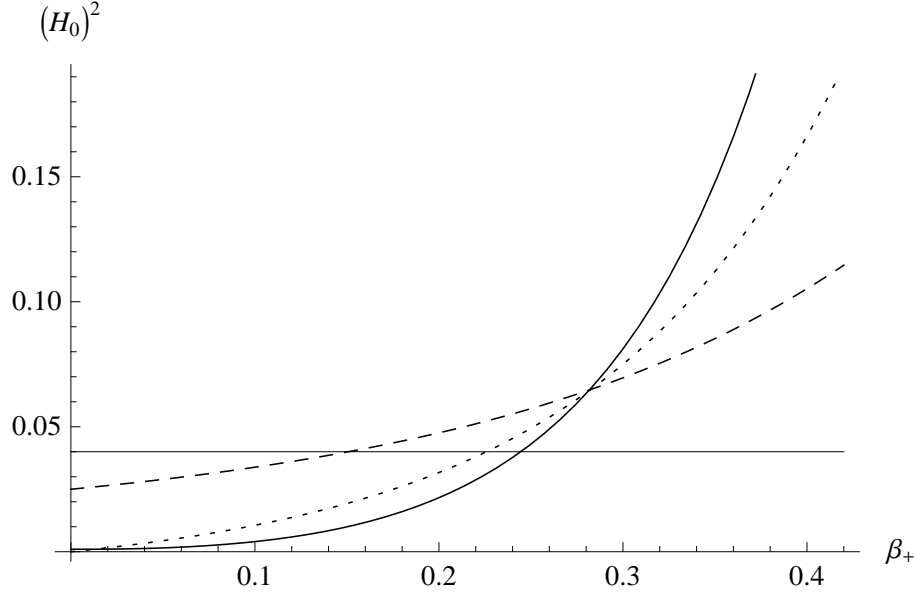


Figure 20: Evolution of second order moments in an expanding universe. $(\Delta\alpha)^2\nu$ (dashed), $(\Delta p_\alpha)^2$ (solid), $\Delta(\alpha p_\alpha)\sqrt{\nu}$ (dotted), with initial values: $(\Delta\alpha)^2\nu = .025H_0^2$, $(\Delta p_\alpha)^2 = .001H_0^2$, $\Delta(\alpha p_\alpha)\sqrt{\nu} = 0$.

Moments

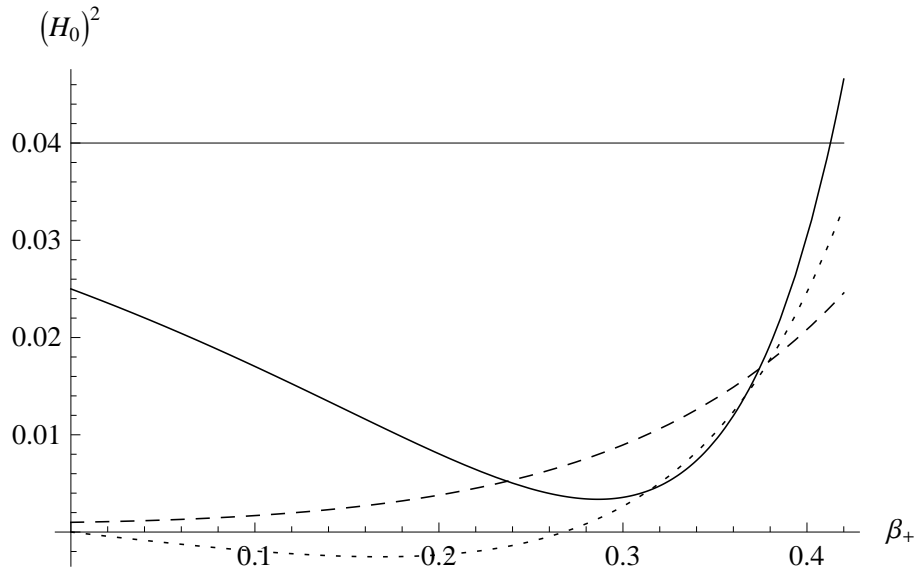


Figure 21: Evolution of second order moments in an expanding universe. $(\Delta\alpha)^2\nu$ (dashed), $(\Delta p_\alpha)^2$ (solid), $\Delta(\alpha p_\alpha)\sqrt{\nu}$ (dotted), with initial values: $(\Delta\alpha)^2\nu = .001H_0^2$, $(\Delta p_\alpha)^2 = .025H_0^2$, $\Delta(\alpha p_\alpha)\sqrt{\nu} = 0$.

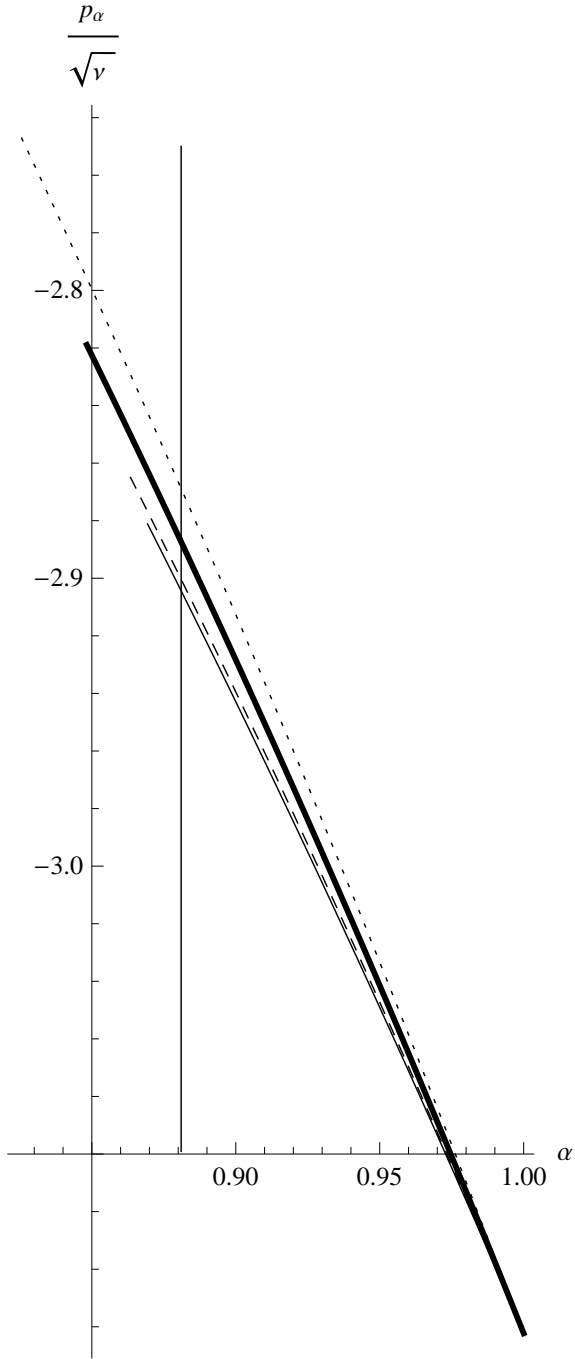


Figure 22: Phase space trajectories of a contracting universe classical (thin solid line) and effective with different initial values for second order moments: dashed line— $(\Delta\alpha)^2\nu = .001H_0^2$, $(\Delta p_\alpha)^2 = .025H_0^2$, $\Delta(\alpha p_\alpha)\sqrt{\nu} = 0$; dotted line— $(\Delta\alpha)^2\nu = .025H_0^2$, $(\Delta p_\alpha)^2 = .001H_0^2$, $\Delta(\alpha p_\alpha)\sqrt{\nu} = 0$; thick solid line— $(\Delta\alpha)^2\nu = .008H_0^2$, $(\Delta p_\alpha)^2 = .008H_0^2$, $\Delta(\alpha p_\alpha)\sqrt{\nu} = .005H_0^2$. Solutions were evolved for $0 < \beta_+ < .07$; the vertical line indicates the breakdown of the semiclassical approximation (coming from the right along the α -axis).

Moments

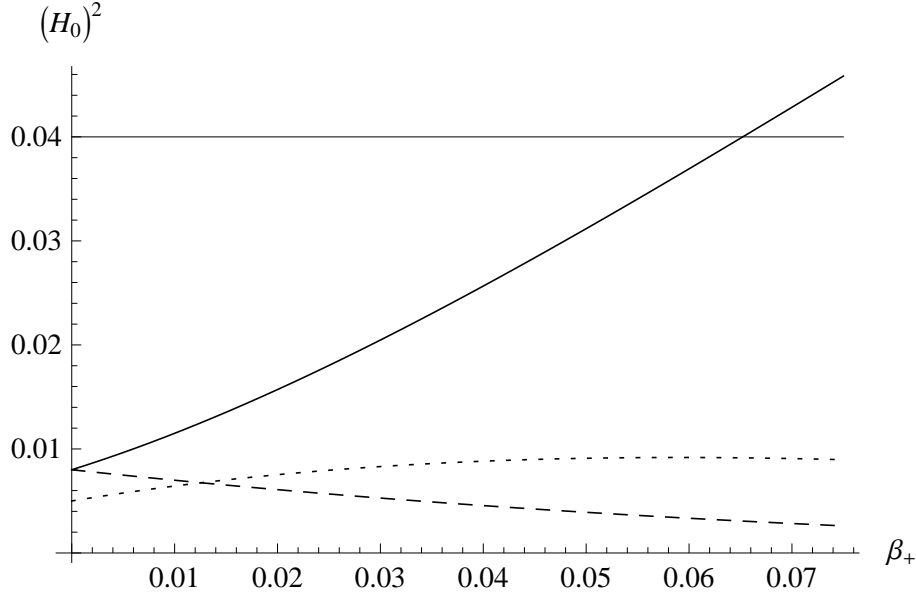


Figure 23: Evolution of second order moments in a contracting universe. $(\Delta\alpha)^2\nu$ (dashed), $(\Delta p_\alpha)^2$ (solid), $\Delta(\alpha p_\alpha)\sqrt{\nu}$ (dotted), with initial values: $(\Delta\alpha)^2\nu = .008H_0^2$, $(\Delta p_\alpha)^2 = .008H_0^2$, $\Delta(\alpha p_\alpha)\sqrt{\nu} = .005H_0^2$.

Moments

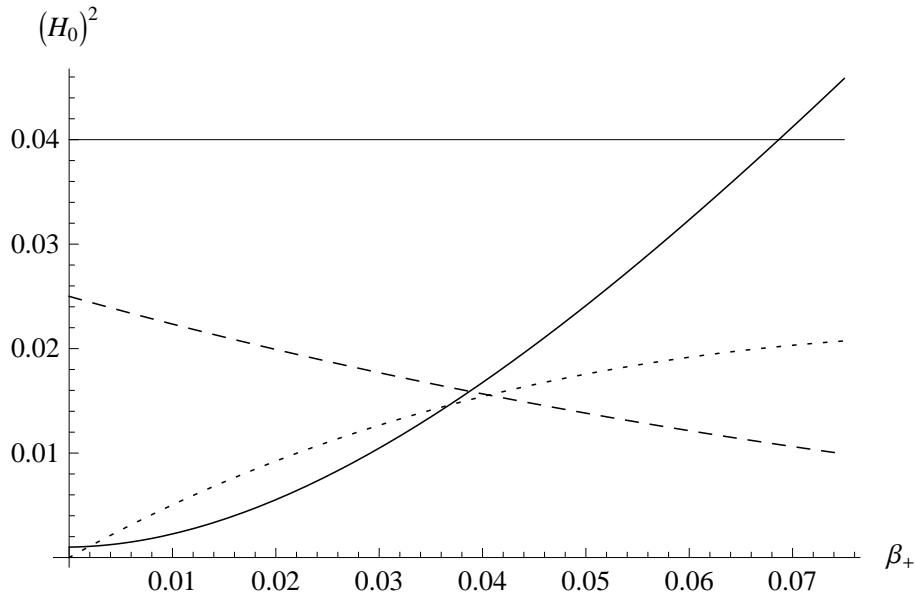


Figure 24: Evolution of second order moments in a contracting universe. $(\Delta\alpha)^2\nu$ (dashed), $(\Delta p_\alpha)^2$ (solid), $\Delta(\alpha p_\alpha)\sqrt{\nu}$ (dotted), with initial values: $(\Delta\alpha)^2\nu = .025H_0^2$, $(\Delta p_\alpha)^2 = .001H_0^2$, $\Delta(\alpha p_\alpha)\sqrt{\nu} = 0$.

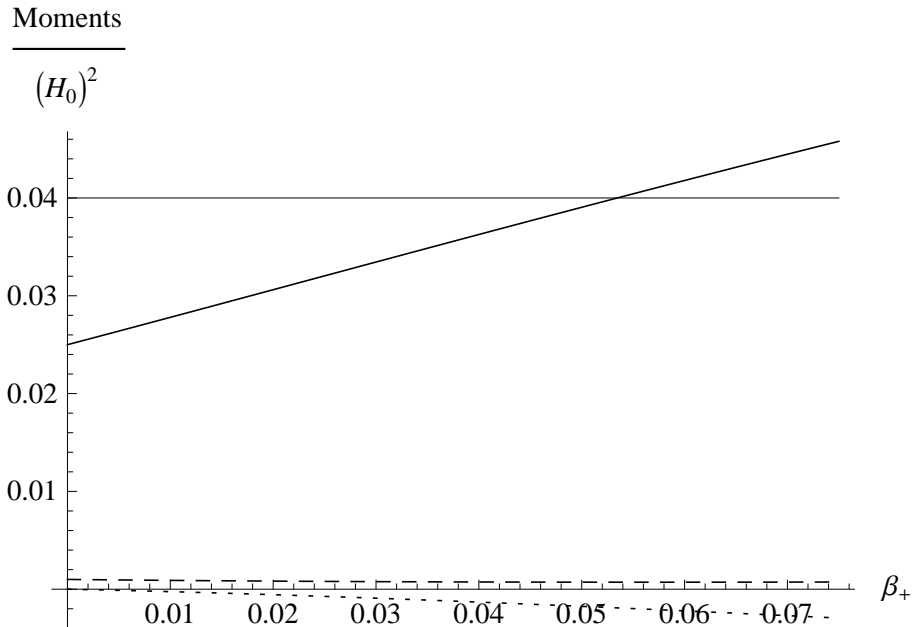


Figure 25: Evolution of second order moments in a contracting universe. $(\Delta\alpha)^2\nu$ (dashed), $(\Delta p_\alpha)^2$ (solid), $\Delta(\alpha p_\alpha)\sqrt{\nu}$ (dotted), with initial values: $(\Delta\alpha)^2\nu = .001H_0^2$, $(\Delta p_\alpha)^2 = .025H_0^2$, $\Delta(\alpha p_\alpha)\sqrt{\nu} = 0$.

5 Conclusions

Most quantum systems of physical relevance can only be analyzed by perturbation methods. Quantum gravity and quantum cosmology cannot be considered exceptions. As demonstrated by the examples of this article, canonical effective equations, based on the back-reaction of moments of a state on its expectation values, are of wide applicability, capture quantum effects reliably, and approximate the full quantum dynamics in a self-consistent way. They are tractable even in situations where semiclassical wave functions in physical Hilbert spaces would be too complicated to be constructed — cases which abound in quantum cosmology and quantum gravity.

Acknowledgements

This work was supported in part by NSF grant PHY 0748336.

References

- [1] F. Cametti, G. Jona-Lasinio, C. Presilla, and F. Toninelli, Comparison between quantum and classical dynamics in the effective action formalism, In *Proceedings of the*

- International School of Physics “Enrico Fermi”, Course CXLIII*, pages 431–448, Amsterdam, 2000. IOS Press, [quant-ph/9910065]
- [2] M. Bojowald and A. Skirzewski, Effective Equations of Motion for Quantum Systems, *Rev. Math. Phys.* 18 (2006) 713–745, [math-ph/0511043]
 - [3] M. Bojowald, Large scale effective theory for cosmological bounces, *Phys. Rev. D* 75 (2007) 081301(R), [gr-qc/0608100]
 - [4] M. Bojowald, Dynamical coherent states and physical solutions of quantum cosmological bounces, *Phys. Rev. D* 75 (2007) 123512, [gr-qc/0703144]
 - [5] M. Bojowald, Quantum nature of cosmological bounces, *Gen. Rel. Grav.* 40 (2008) 2659–2683, [arXiv:0801.4001]
 - [6] M. Bojowald, B. Sandhöfer, A. Skirzewski, and A. Tsobanjan, Effective constraints for quantum systems, *Rev. Math. Phys.* 21 (2009) 111–154, [arXiv:0804.3365]
 - [7] M. Bojowald and A. Tsobanjan, Effective constraints for relativistic quantum systems, *Phys. Rev. D* (2009) to appear, [arXiv:0906.1772]
 - [8] C. W. Misner, Mixmaster Universe, *Phys. Rev. Lett.* 22 (1969) 1071–1074
 - [9] J. B. Hartle and D. Marolf, Comparing Formulations of Generalized Quantum Mechanics for Reparametrization-Invariant Systems, *Phys. Rev. D* 56 (1997) 6247–6257, [gr-qc/9703021]
 - [10] G. Barnich and M. Grigoriev, Hamiltonian BRST and Batalin–Vilkovisky formalisms for second quantization of gauge theories, *Commun. Math. Phys.* 254 (2005) 581–601, [hep-th/0310083]